

Kinematic space for conical defects

Jesse C. Cresswell^a Amanda W. Peet^{a,b}

^a*Department of Physics, University of Toronto,
60 St. George St., Toronto, Canada*

^b*Department of Mathematics, University of Toronto,
40 St. George St., Toronto, Canada*

E-mail: jcresswe@physics.utoronto.ca, awpeet@physics.utoronto.ca

ABSTRACT: Kinematic space can be used as an intermediate step in the AdS/CFT dictionary and lends itself naturally to the description of diffeomorphism invariant quantities. From the bulk it has been defined as the space of boundary anchored geodesics, and from the boundary as the space of pairs of CFT points. When the bulk is not globally AdS₃ the appearance of non-minimal geodesics leads to ambiguities in these definitions. In this work conical defect spacetimes are considered as an example where non-minimal geodesics are common. From the bulk it is found that the conical defect kinematic space can be obtained from the AdS₃ kinematic space by the same quotient under which one obtains the defect from AdS₃. The resulting kinematic space is one of many equivalent fundamental regions. From the boundary the conical defect kinematic space can be determined by breaking up OPE blocks into contributions from individual bulk geodesics. A duality is established between partial OPE blocks and bulk fields integrated over individual geodesics, minimal or non-minimal.

KEYWORDS: AdS-CFT Correspondence, Gauge-gravity correspondence, Conformal Field Theory

ARXIV EPRINT: [1708.09838](https://arxiv.org/abs/1708.09838)

Contents

1	Introduction	1
2	Kinematic space from the bulk	3
2.1	Review of geometries	3
2.2	Kinematic space from differential entropy	5
2.3	Kinematic space from boundary anchored geodesics	7
3	Kinematic space from the boundary	9
3.1	Kinematic space metric from conformal symmetry	9
3.2	OPE blocks	10
3.3	CFT dual to conical defects	14
3.3.1	Partial OPE block decomposition	15
3.3.2	Partial OPE block Casimir equations	18
4	Discussion	20
4.1	Duality between OPE blocks and geodesic integrals of bulk fields	21
4.2	Future directions	27

1 Introduction

Even before the AdS/CFT correspondence [1–3] provided a physical duality between conformal field theories and theories of quantum gravity in Anti-de Sitter spacetimes, CFT quantities had been mathematically represented in terms of bulk fields [4, 5]. These ideas relating contributions to conformal blocks and integrals of bulk fields over geodesics have reemerged recently in the context of geodesic Witten diagrams [6, 7]. Whereas a four-point Witten diagram with bulk vertices integrated over the entire bulk calculates a full CFT four-point function, integrating the vertices only over geodesics connecting boundary insertions computes a conformal partial wave. The conformal partial wave represents the contribution of a primary operator and its descendants to the four-point function, and somehow knows about the geodesic structure of AdS.

A new approach to the AdS/CFT correspondence has shed more light on the connection between composite operators in the operator product expansion (OPE), and integrated bulk fields. The authors of [8, 9] proposed the use of an auxiliary space that interpolates between the bulk and boundary theories, similar to the space used in [10]. The auxiliary space, called kinematic space, functions as a way of organizing the non-local degrees of freedom which lead to diffeomorphism invariant quantities in the bulk gravity theory. Whereas local bulk fields fail to satisfy diffeomorphism invariance, a field integrated over a boundary anchored geodesic or otherwise attached to the boundary with a geodesic dressing can be

invariant [11, 12]. Boundary anchored geodesics in asymptotically AdS spacetimes meet the boundary at pairs of spacelike or null separated points suggesting a relation to bi-local CFT operators. Such composite operators are easily described in terms of the OPE. Both a geodesic integrated field and the basis of non-local operators forming the OPE can be viewed as fields on kinematic space leading to a diffeomorphism invariant entry into the AdS/CFT dictionary.

Several proposals have been made as to how kinematic space should be defined from the bulk and boundary. Kinematic space was originally presented as the space of bulk geodesics with a measure derived from their lengths in terms of the Crofton form [8]. Since the length of a minimal geodesic is holographically related to entanglement entropy in AdS₃/CFT₂ [13], a boundary description of kinematic space was given as the space of boundary intervals with the metric defined in terms of the differential entropy of those intervals [14].¹ In order to generalize the kinematic space approach to higher dimensional systems, later approaches defined points in kinematic space as oriented bulk geodesics, and simultaneously as ordered pairs of boundary points [9].

In the case of a pure AdS₃ geometry, these approaches are consistent since there is a unique geodesic connecting each pair of spacelike separated boundary points. Other well known locally AdS₃ geometries can have several geodesics connecting each pair of boundary points, namely conical defects and the BTZ black holes [16–18]. There are two diverging ways to modify the definition of what constitutes a kinematic space point in such cases. Any spacelike separated pair of boundary points will be connected by a unique minimal geodesic, so the bulk definition can exclude non-minimal geodesics from kinematic space with no need to change the boundary definition. Alternatively, non-minimal geodesics can be considered as points with the same standing as minimal ones, in which case ordered pairs of boundary points alone will not fill out kinematic space. Excluding non-minimal geodesics is not desirable due to the generic fact that minimal geodesics do not reach all depths of the bulk. The region probed by non-minimal geodesics is known as the entanglement shadow [19–21]. A full description of the bulk in terms of kinematic space can only succeed when non-minimal geodesics are included. This forces a change to the definition of kinematic space from the boundary point of view.

In this paper, we take up the issue of non-minimal geodesics in kinematic space, and the matter of an equivalent boundary definition of points in the simplest geometry exhibiting this feature, the static conical defects in three bulk dimensions. In section 2 the geometry of the conical defect kinematic space is derived in two ways. The first is a simple application of the differential entropy definition applied to geodesics of all lengths. The second follows [22] in noting that the conical defects can be obtained as a quotient of pure AdS₃. Under this quotient classes of geodesics are identified, producing a quotient on kinematic space, and leading to a result equivalent to the first approach. In section 3 the metric of kinematic space is extracted from OPE blocks in the CFT. By mapping to a convenient covering CFT system we find that conventional OPE blocks can be broken down further than done before

¹This approach was recently inverted to derive the universal parts of the entanglement entropy in a CFT with a boundary from knowledge of the kinematic space [15].

using the method of images. Individual image contributions to the OPE blocks contain information about subregions of kinematic space that, when combined, reproduce the same space identified from the bulk. Intuition from previous uses of the method of images to calculate correlation functions holographically suggests an association between partial OPE blocks in the CFT and geodesics of a fixed winding number in the bulk. Kinematic space provides a realm where the connection between these objects can be made precise, as is shown in section 4. We conclude by isolating the contribution to the full OPE block from individual bulk geodesics, minimal or non-minimal, connecting the boundary insertion points. This extends the holographic dictionary established in [9] between OPE blocks and geodesic integrated operators, and provides more fine-grained information about the holographic contributions to the blocks.

To help visualize the physics on the conical defect, covering space, and kinematic space, an interactive Mathematica demonstration is provided with this paper as an ancillary file. It does not require a Mathematica license to be used.

2 Kinematic space from the bulk

In this section we focus on static conical defect spacetimes and consider the kinematic space for a constant time slice. We show that the differential entropy approach [8], and the quotient approach [22] produce different fundamental regions of the same kinematic space, but are entirely equivalent.

2.1 Review of geometries

In global coordinates, the universal cover of AdS_3 has the metric

$$ds^2 = R_{\text{AdS}}^2(-\cosh^2 \rho dt^2 + d\rho^2 + \sinh^2 \rho d\phi^2), \quad (2.1)$$

with $t \in \mathbb{R}$, $\rho \in \mathbb{R}^+$, and $\phi \in [0, 2\pi]$ with the identification $\phi = \phi + 2\pi$. Throughout this paper the “unwrapped” time coordinate t of the universal cover will be used. The AdS_3 geometry can be understood as a surface embedded in the higher dimensional flat space $\mathbb{R}^{(2,2)}$ with metric

$$ds^2 = -dU^2 - dV^2 + dX^2 + dY^2. \quad (2.2)$$

The AdS_3 metric is induced by restricting to a hyperbolic surface

$$-U^2 - V^2 + X^2 + Y^2 = -R_{\text{AdS}}^2. \quad (2.3)$$

The parameter R_{AdS} is the AdS length scale which will be set to unity throughout the remainder of this paper. The metric in global coordinates is obtained from the embedding equations

$$U = \cosh \rho \cos t, \quad V = \cosh \rho \sin t, \quad X = \sinh \rho \cos \phi, \quad Y = \sinh \rho \sin \phi. \quad (2.4)$$

For visual representations it will be useful to consider the Poincaré disk. By taking a constant time slice $t = 0$, equivalently $V = 0$, the metric induced from $\mathbb{R}^{(1,2)}$ is that of the hyperbolic plane \mathbb{H}_2 ,

$$ds^2 = d\rho^2 + \sinh^2 \rho d\phi^2. \quad (2.5)$$

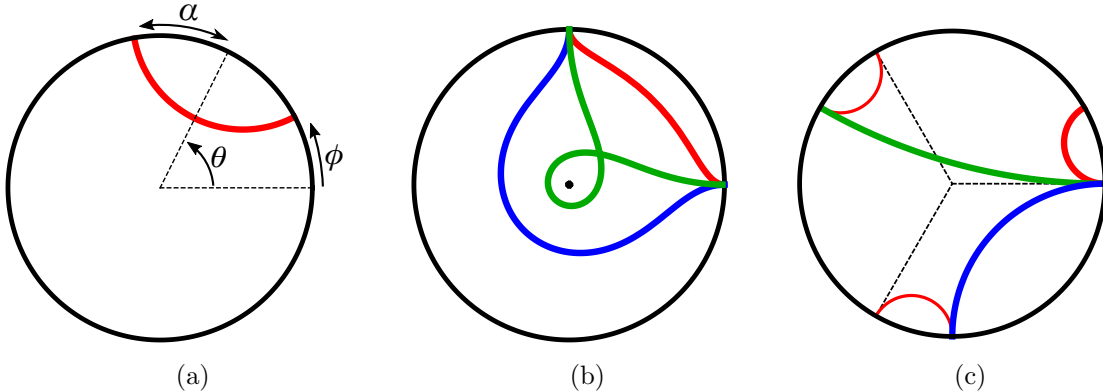


Figure 1: (a) The Poincaré disk showing a geodesic and its kinematic coordinates. (b) A spatial slice of a conical defect, with $N = 3$ for illustration, showing three geodesics subtending the same boundary interval with winding numbers $n = 0, 1, 2$ respectively in order of increasing length. (c) The covering space of the conical defect showing identified wedges, and preimages of the corresponding geodesics in figure (b). Also shown are two equivalent images of the minimal geodesic (red).

This describes a two sheeted hyperboloid in $\mathbb{R}^{(1,2)}$ with disconnected parts above and below the $U = 0$ plane. The tips of the sheets are located at $(-1, 0, 0)$ and $(1, 0, 0)$ in the (U, X, Y) embedding coordinates. The Poincaré disk can be obtained by projecting the $U > 1$ sheet onto the $U = 0$ plane through the point $(-1, 0, 0)$. In the disk, boundary anchored geodesics are described by the particularly simple equation

$$\tanh \rho \cos(\phi - \theta) = \cos \alpha. \quad (2.6)$$

Here θ denotes the angular coordinate of the center of the geodesic, and $\alpha \in [0, \pi]$ is the half-opening angle. Pictorially, geodesics in the Poincaré disk are arcs of circles that meet the boundary at right angles as in figure 1a.

Conical defect spacetimes can be obtained as a quotient of AdS_3 by identifying surfaces of constant ϕ leaving an angular coordinate with a smaller period. In global coordinates the metric is simply

$$ds^2 = -\cosh^2 \rho dt^2 + d\rho^2 + \sinh^2 \rho d\tilde{\phi}^2, \quad (2.7)$$

where now $\tilde{\phi} = \tilde{\phi} + \frac{2\pi}{N}$. The parameter $N \in (1, \infty)$ gives the strength of the defect. This metric is no longer a solution of the vacuum Einstein equations everywhere but requires a pointlike source at the origin. The defect can be viewed as a static particle of mass M where $4G_N M = 1 - 1/N$. The mass must stay below the black hole limit $M = 1/4G_N$, which corresponds to $N \rightarrow \infty$. For the special cases where N is an integer, the spacetime is a cyclic orbifold $\text{AdS}_3/\mathbb{Z}_N$. Some example geodesics in the $t = 0$ slice of the conical defect are shown in figure 1b, and the corresponding geodesics of AdS_3 in figure 1c.

The kinematic space corresponding to the Poincaré disk was investigated in [8] and found to be a two dimensional de-Sitter geometry. For ease of comparison the dS_2 spacetime can be embedded in the same $\mathbb{R}^{(1,2)}$ where it is a one-sheeted hyperboloid given by

$$-U^2 + X^2 + Y^2 = 1. \quad (2.8)$$

The embedding equations

$$U = \sinh t, \quad X = \cosh t \cos \theta, \quad Y = \cosh t \sin \theta, \quad (2.9)$$

lead to the dS₂ metric in global coordinates,

$$ds^2 = -dt^2 + \cosh^2 t d\theta^2. \quad (2.10)$$

Conformal or “kinematic” coordinates (α, θ) will be used often in this paper as they naturally fit with the description of kinematic space as the space of geodesics in AdS₃. The transformation $\cosh t = 1/\sin \alpha$, where now $\alpha \in [0, \pi]$, leads to the dS₂ metric

$$ds^2 = \frac{-d\alpha^2 + d\theta^2}{\sin^2 \alpha}. \quad (2.11)$$

With these conventions laid out, the remainder of this section briefly recounts the derivation of the kinematic space geometry for pure AdS₃, then details two methods of obtaining the kinematic space for conical defects from the bulk.

2.2 Kinematic space from differential entropy

In [8] a definition of kinematic space for constant time slices of AdS₃ in terms of differential entropy was derived from integral geometry. Each interval of the boundary, denoted by an ordered pair of points (u, v) , corresponds to a point in kinematic space covered by null coordinates (u, v) . The kinematic space metric in these coordinates was found to be

$$ds^2 = \frac{\partial^2 S(u, v)}{\partial u \partial v} du dv, \quad (2.12)$$

where $S(u, v)$ was the length of the shortest oriented geodesic connecting the ends of the interval (u, v) through the bulk. Since the length of a minimal geodesic is holographically interpreted as the entanglement entropy of the interval it subtends, the quantity $\partial^2 S/\partial u \partial v$ was dubbed differential entropy [13, 14, 23, 24]. However, many interesting spacetimes including the conical defects and BTZ black holes have multiple geodesics connecting pairs of spacelike separated boundary points. Non-minimal geodesics do not correspond to entanglement between spatial regions, but have been conjectured to describe correlations between internal degrees of freedom [19]. Because of this potential interest, and their importance in the geodesic approximation for correlation functions [25, 26], in this paper the differential entropy definition will be expanded to include non-minimal geodesics.

For the constant time slice of AdS₃, there is a unique oriented geodesic connecting each ordered pair of boundary points so the issue of non-minimal geodesics in eq. (2.12) does not arise. Geodesics can be labelled by their half-opening angle α and centre angle θ , and have length

$$S(\alpha) = \frac{1}{2G_N} \log \frac{2 \sin \alpha}{\mu}, \quad (2.13)$$

where μ serves as a gravitational infrared cutoff [27]. By transforming between kinematic coordinates and null coordinates using $u = \theta - \alpha$, and $v = \theta + \alpha$, eq. (2.12) can be applied

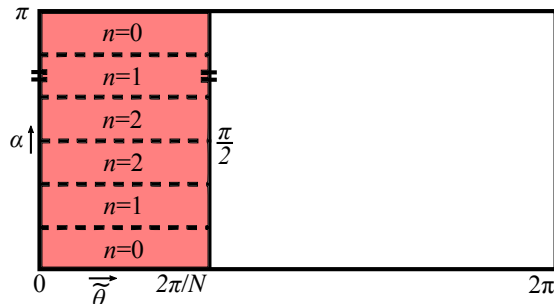


Figure 2: The Penrose diagram for the dS_2 kinematic space for pure AdS_3 is shown as the full rectangular region, with $\theta = \theta + 2\pi$. For the conical defect case the differential entropy definition of kinematic space produces a vertical strip subregion. The same angular identification which gives the conical defect from AdS_3 also gives the kinematic space. $N = 3$ is shown for illustration throughout most of this paper.

to find

$$\begin{aligned}
 ds^2 &= \frac{1}{8G_N} \frac{1}{\sin^2[(v-u)/2]} dudv \\
 &= \frac{1}{8G_N} \frac{-d\alpha^2 + d\theta^2}{\sin^2 \alpha}.
 \end{aligned} \tag{2.14}$$

Thus, the kinematic space of a constant time slice of AdS_3 is dS_2 according to the differential entropy definition, as shown in figure 2. The $\alpha < \pi/2$ and $\alpha > \pi/2$ halves are mapped into one another under orientation reversal which acts as $\alpha \rightarrow \pi - \alpha$ and $\theta \rightarrow \theta + \pi$. The geodesics with $\alpha = \pi/2$ cut straight across the Poincaré disk and have maximal length.

Now consider a constant time slice of the conical defect geometry eq. (2.7). Since the total angle around the boundary is $2\pi/N$, the centre angle of a geodesic will now be denoted $\tilde{\theta} \in [0, 2\pi/N]$. Once again, for any pair of boundary points there is a unique minimal geodesic connecting them through the bulk. Minimal geodesics have half-opening angles in the domain $\alpha \in [0, \pi/2N]$, and by reversing orientations with $\alpha \rightarrow \pi - \alpha$ and $\tilde{\theta} \rightarrow \tilde{\theta} + \pi/N$, also the domain $\alpha \in [(2N-1)\pi/2N, \pi]$. Minimal geodesics cover the top and bottom regions of kinematic space in figure 2.

In contrast to AdS_3 , there can be non-minimal geodesics connecting pairs of boundary points. It will be useful to label geodesics and their corresponding regions in kinematic space by the number of times they wind around the defect, n . The cases of integer and non-integer N will be treated separately for clarity.

For integer N there are $N - 1$ non-minimal geodesics connecting each pair of boundary points, with winding numbers $1 \leq n \leq N - 1$. Geodesics with winding number n fill in the regions of kinematic space

$$\alpha \in \left(\frac{n\pi}{2N}, \frac{(n+1)\pi}{2N} \right], \quad \alpha \in \left[\frac{(2N-n-1)\pi}{2N}, \frac{(2N-n)\pi}{2N} \right), \tag{2.15}$$

where these domains are related by orientation reversal. The upper and lower halves of kinematic space are divided by geodesics with $\alpha = \pi/2$ which touch the conical defect. On

the covering AdS₃ space, these are the straight lines through the origin of the Poincaré disk. In total there are $2N$ equally sized regions on kinematic space in the $(\alpha, \tilde{\theta})$ coordinates.

For non-integer N , the maximally winding geodesics have $n = \lfloor N \rfloor$ and live near the centre line $\alpha = \pi/2$. There are fewer maximally winding geodesics than other classes, filling out a truncated region

$$\alpha \in \left(\frac{(\lfloor N \rfloor - 1)\pi}{2N}, \frac{(\lfloor N \rfloor + 1)\pi}{2N} \right). \quad (2.16)$$

Other winding numbers follow eq. (2.15). Each pair of boundary points is connected by $\lfloor N \rfloor$ or $\lfloor N \rfloor - 1$ geodesics, depending on their angular separation.

The differential entropy definition eq. (2.12) can be applied to show that the geometry on kinematic space remains locally dS₂ for any N . The key fact is that minimal and non-minimal geodesics still have lengths given by eq. (2.13) [27]. Treating the types on equal footings from the point of view of kinematic space and using $u = \tilde{\theta} - \alpha$, $v = \tilde{\theta} + \alpha$ once again gives²

$$ds^2 = \frac{1}{8G_N} \frac{-d\alpha^2 + d\tilde{\theta}^2}{\sin^2 \alpha}. \quad (2.17)$$

The kinematic space for a constant time slice of a conical defect has the same dS₂ metric as the AdS₃ case, but with the angular coordinate identified as $\tilde{\theta} \sim \tilde{\theta} + 2\pi/N$. This was expected since the static conical defects are locally AdS₃, only differing by the global identification along the angular coordinate. The identification does not affect the lengths of the remaining geodesics. From the differential entropy perspective, the conical defect kinematic space is found by taking an angular quotient of the AdS₃ kinematic space; the same quotient that produces the conical defect from pure AdS₃ itself. In the next section we show how the quotient acts on geodesics in the covering space, displaying the inherent ambiguities involved in defining kinematic space.

2.3 Kinematic space from boundary anchored geodesics

The bulk calculation of the kinematic space for conical defects is more enlightening when the defects are viewed from the perspective of the covering space, AdS₃. In particular, it provides motivation for treating minimal and non-minimal geodesics on equal footing in the definition of kinematic space, since there is no real distinction between the types when viewed in the cover. All spacelike geodesics of the conical defect descend from the covering space; the quotient that produces the conical defect divides geodesics into equivalence classes.

As an explicit example, consider the case of $N = 2$. The covering space of $\mathbb{H}_2/\mathbb{Z}_2$ is shown in figure 3a. The covering space can be split into two regions with boundaries labelled A and B , which are identified under the quotient. Boundary anchored geodesics on this slice can be grouped into four classes $\{AA, BB, AB, BA\}$ depending on the boundary

²A previous paper [28] describing the kinematic spaces for several locally AdS₃ geometries, including conical defects, chose to consider only minimal geodesics, and hence found different kinematic space geometries.

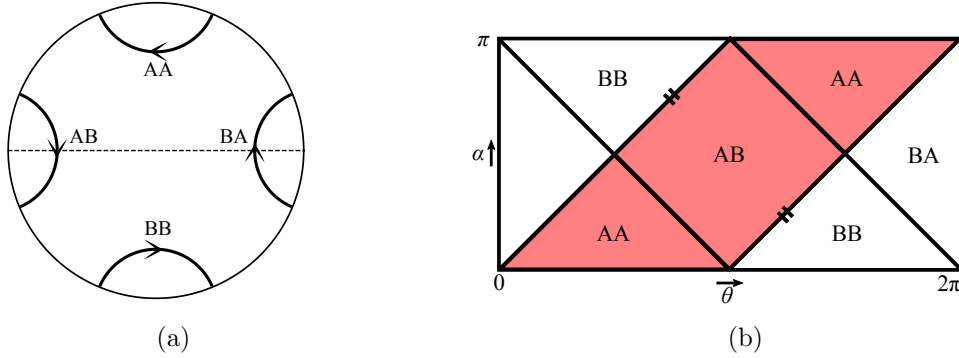


Figure 3: (a) Oriented geodesics in the Poincaré disk labelled by their endpoint locations. The $N = 2$ wedges are shown with two identified boundaries A and B. (b) Regions of kinematic space labelled by the boundaries each geodesic ends on. For the conical defect with $N = 2$, the shaded diagonal strip is a fundamental domain equivalent to the vertical strip.

region their endpoints lie on. The locations of the classes on kinematic space are shown in figure 3b.

Under the \mathbb{Z}_2 quotient, BB geodesics are mapped into AA geodesics. Similarly, BA geodesics are mapped into AB geodesics. Therefore, all geodesics in $\mathbb{H}_2/\mathbb{Z}_2$ can be generated by the classes $\{AA, AB\}$, and the \mathbb{Z}_2 action. The number of unique geodesics in the conical defect slice is greatly reduced, and similarly for points on kinematic space. As is shown in figure 3b, the kinematic space for the $N = 2$ conical defect slice is a diagonal strip of width $\theta = \pi$, with the identification $\theta = \theta + \pi$. However, there are many equivalent ways to choose the fundamental region under the quotient action. If, for example, the classes $\{AA, BA\}$ had been chosen as fundamental, the diagonal strip would point in the opposite direction. Similarly, the entire strip can be shifted by any amount in the θ direction. There is nothing to distinguish these choices, so as in [22] a conventional choice has been made.

The quotient only changes the global identification of points in the spacetime, and the geodesics within it. The relationship between nearby geodesics in the kinematic space metric are locally unchanged. While the origin of AdS_3 is a fixed point of the quotient, there are no oriented geodesics which are left invariant. From the perspective of kinematic space, the quotient is freely acting, so the metric is expected to be locally unchanged, and the topology to be invariant. This is in contrast to the kinematic space of the BTZ black hole found in [22]. The quotient of AdS_3 which produces a BTZ black hole has no fixed points so there are no curvature singularities in the BTZ spacetime, but there are geodesics which are fixed under the quotient which changes the topology of kinematic space from a single cylinder to two.

For the more general case of a \mathbb{Z}_N quotient, there are N^2 distinct classes of oriented geodesics from the number of ways we can choose two ordered endpoints. The number of distinct regions in kinematic space is $N(N + 1)$, one for each of the N^2 classes, and one extra for each of the N boundaries. The fundamental region is a diagonal strip with width given by $2\pi/N$ since $\theta = \theta + 2\pi/N$ is identified. This also describes the fundamental region for arbitrary N .

The two approaches presented here, using the differential entropy definition eq. (2.12), and studying how the quotient identifies geodesics on the covering space both produce a locally dS_2 spacetime but naturally pick out different regions of the kinematic space. The differential entropy definition picks out a vertical strip, while the classification of endpoints on the covering space produces a diagonal strip. However, it is clear from the latter approach that there are many equivalent choices of fundamental region, each with its own merits. The diagonal choice contains some geodesics which have boundary position $\theta > 2\pi/N$ on the cover. The vertical choice only contains geodesics which are centred at boundary coordinates $\theta < 2\pi/N$. Since it is easiest to label geodesics with kinematic coordinates $\alpha \in (0, \pi)$ and $\tilde{\theta} \in [0, 2\pi/N]$, the vertical strip will be used in the rest of this paper.

3 Kinematic space from the boundary

3.1 Kinematic space metric from conformal symmetry

In [9] a definition of kinematic space from the boundary theory was given: each point in kinematic space corresponds to an ordered pair of CFT points.³ For pure AdS_3/CFT_2 restricted to a time slice, each ordered pair of CFT points singles out a unique spacelike boundary anchored geodesic so this definition is entirely natural. In the full time dependent geometry, conformal symmetry alone fixes the metric on kinematic space to be

$$ds^2 = 4 \frac{I_{\mu\nu}(x_1 - x_2)}{|x_1 - x_2|^2} dx_1^\mu dx_2^\nu, \quad (3.1)$$

where

$$I_{\mu\nu}(x_1 - x_2) = \eta_{\mu\nu} - 2 \frac{(x_1 - x_2)_\mu (x_1 - x_2)_\nu}{(x_1 - x_2)^2}, \quad (3.2)$$

is the inversion tensor. The numerical prefactor in the metric is chosen by convention. The two CFT points x_1^μ and x_2^μ form a pair of lightlike coordinates on kinematic space with the strange signature $(2, 2)$. Since kinematic space is not to be viewed as a physical space, but only as a useful auxiliary space for translating between the bulk and boundary, this is not a concern.

In order to get back the dS_2 metric found from the bulk, it is easiest to perform a coordinate transformation from the planar set $x_1^\mu = \{t_1, x_1\}$ to kinematic coordinates on the cylinder. The two pairs of kinematic coordinates are defined through

$$\begin{aligned} \tan \alpha &= \frac{1}{2} (t_1 - t_2 + x_1 - x_2), & \theta &= \frac{1}{2} (t_1 + t_2 + (x_1 + x_2)), \\ \tan \bar{\alpha} &= \frac{1}{2} (t_1 - t_2 - (x_1 - x_2)), & \bar{\theta} &= \frac{1}{2} (t_1 + t_2 - (x_1 + x_2)). \end{aligned} \quad (3.3)$$

In terms of these coordinates the kinematic space metric is two copies of the dS_2 metric in eq. (2.11),

$$ds^2 = \frac{-d\alpha^2 + d\theta^2}{2 \sin^2 \alpha} + \frac{-d\bar{\alpha}^2 + d\bar{\theta}^2}{2 \sin^2 \bar{\alpha}}. \quad (3.4)$$

³In [9] and [29] it was shown that an equivalent definition can be made in terms of boundary causal diamonds.

Thus the kinematic space for global AdS₃, and the dual vacuum state of a CFT₂ is dS₂ × dS₂. When we restrict to a constant time slice by setting $t_1 = t_2 = 0$ we see from eq. (3.3) that $\bar{\alpha}$ and $\bar{\theta}$ become redundant coordinates fixed in terms of $\{\alpha, \theta\}$, and that eq. (3.4) becomes eq. (2.17), up to the arbitrarily chosen prefactor.

When the bulk spacetime has non-minimal geodesics, there is no longer a one-to-one correspondence between pairs of CFT points and bulk geodesics. In such a case the argument above cannot be applied. In order to reproduce the quotient structure of kinematic space for conical defects seen in section 2, another approach must be taken. We take the point of view espoused in [30]; OPE blocks in the CFT should be viewed as free fields on kinematic space, and their equation of motion reflects the geometry of kinematic space.

3.2 OPE blocks

In [9], the operator product expansion (OPE) of two scalar CFT operators was broken into OPE blocks, and these blocks were identified as fields on kinematic space. Two scalar operators $\mathcal{O}_i(x_1)$ and $\mathcal{O}_j(0)$ in a planar CFT with conformal weights Δ_i and Δ_j respectively can be expanded in terms of a local basis of operators at the origin,

$$\mathcal{O}_i(x)\mathcal{O}_j(0) = \sum_k C_{ijk} |x|^{\Delta_k - \Delta_i - \Delta_j} (1 + b_1 x^\mu \partial_\mu + b_2 x^\mu x^\nu \partial_\mu \partial_\nu + \dots) \mathcal{O}_k(0). \quad (3.5)$$

This is the OPE, where the quasiprimaries $\mathcal{O}_k(0)$, and their descendants given by the derivative terms, form the basis of operators at the origin. Notably, the b_n coefficients are completely fixed by conformal symmetry, while the C_{ijk} are simply constants, but are theory-dependent. Each term in the sum has a characteristic scaling dimension Δ_k , the dimension of the quasiprimary \mathcal{O}_k , and represents the contribution to the OPE of the entire conformal family of \mathcal{O}_k . Each of these terms can be packaged into a new operator $\mathcal{B}_k^{ij}(x_1, x_2)$ called an OPE block, and the OPE can be written as

$$\mathcal{O}_i(x_1)\mathcal{O}_j(x_2) = |x_1 - x_2|^{-\Delta_i - \Delta_j} \sum_k C_{ijk} \mathcal{B}_k^{ij}(x_1, x_2). \quad (3.6)$$

Since the OPE blocks depend on a pair of CFT points, the two points where operators in the OPE are inserted, it is natural to view them as fields on kinematic space. A major insight of [9] was that the Casimir eigenvalue equation satisfied in the CFT by the OPE blocks can be interpreted as a wave equation. The differential representation of the CFT Casimir operator appropriate for OPE blocks is the Laplacian in the kinematic space metric eq. (3.4). This gives yet another prescription for determining the kinematic space for a CFT state which is applicable when arguments from conformal symmetry alone are not sufficient, as advocated for recently in [30]. In the following section, we will show how this prescription can be modified and used to obtain the kinematic space for excited CFT states dual to conical defects, in agreement with the results of section 2. First, we review how the bulk metric of AdS₃ can be determined from a quadratic CFT₂ Casimir in a differential representation appropriate for scalar fields, and how the bilocal scalar representation of OPE blocks gives the metric on kinematic space. These initial cases have been summarized in [9, 29].

In a 2d CFT, the global conformal group $SO(2, 2)$ forms a subgroup of the larger Virasoro symmetry group. The global subgroup corresponds holographically to the isometries of pure AdS_3 with appropriate boundary conditions, while the other generators of the Virasoro group are associated to transformations which preserve the asymptotic boundary [31]. The global conformal generators $L_{0,\pm 1}$, $\bar{L}_{0,\pm 1}$ in the standard basis satisfy two copies of the Witt algebra

$$[L_n, L_m] = (n - m)L_{n+m}, \quad [\bar{L}_n, \bar{L}_m] = (n - m)\bar{L}_{n+m}, \quad [L_n, \bar{L}_m] = 0. \quad (3.7)$$

When acting on conformal operators, the algebra is represented by some differential operators \mathcal{L}_n as

$$[L_n, \mathcal{O}_k(x)] = \mathcal{L}_n \mathcal{O}_k(x), \quad (3.8)$$

which depend on the $SO(2, 2)$ representation of \mathcal{O}_k .

The quadratic Casimir operator

$$\mathcal{C}_2 = -\frac{1}{2}L^{AB}L_{AB} = -2L_0^2 + (L_1L_{-1} + L_{-1}L_1) + (L \rightarrow \bar{L}), \quad (3.9)$$

commutes with all the global conformal generators.⁴ Here, L_{AB} is written as an $SO(2, 2)$ Lorentz operator in the embedding space formalism [32]. Quasiprimary operators $\mathcal{O}_k(x)$ are eigenoperators of this Casimir obeying

$$[\mathcal{C}_2, \mathcal{O}_k(x)] = -\frac{1}{2}\mathcal{L}^{AB}\mathcal{L}_{AB}\mathcal{O}_k(x) = C_k\mathcal{O}_k(x), \quad (3.10)$$

where for a quasiprimary with scaling dimension Δ_k and spin l_k the eigenvalue is

$$C_k = \Delta_k(\Delta_k - d) - l_k(l_k + d - 2). \quad (3.11)$$

The same eigenvalue applies to the conformal Casimir in higher dimensional CFT's although we only consider $d = 2$ here. Since descendants of $\mathcal{O}_k(x)$ are obtained through the action of conformal generators which commute with \mathcal{C}_2 , descendants obey the same Casimir eigenvalue equation. Thus, Casimir eigenvalues classify irreducible representations of the global conformal group.

The holographic interpretation of the Casimir equation (3.10) depends on the representation used for the conformal generators. As an example, consider a scalar quasiprimary operator \mathcal{O}_k with dimension Δ_k , dual to a massive bulk scalar field φ . In terms of right and left moving planar CFT coordinates $\xi = x + t$, $\bar{\xi} = x - t$, the appropriate differential representation of the global conformal generators is

$$\mathcal{L}_{-1} = \partial_\xi, \quad \mathcal{L}_0 = -\xi\partial_\xi - \frac{1}{2}\Delta_k, \quad \mathcal{L}_1 = \xi^2\partial_\xi + \xi\Delta_k, \quad (3.12)$$

and similarly for barred generators with $\xi \rightarrow \bar{\xi}$. An explicit calculation of eq. (3.10) using eq. (3.9) verifies that $[\mathcal{C}_2, \mathcal{O}_k(x)] = \Delta_k(\Delta_k - 2)\mathcal{O}_k(x)$.

⁴Our conventions are as in [29].

Holographically, the global conformal generators correspond with AdS₃ isometries. Scale/radius duality prescribes that the scaling dimension Δ_k be replaced by the radial scale operator $z\partial_z$. Then the conformal generators become

$$\eta_{-1} = \partial_\xi, \quad \eta_0 = -\xi\partial_\xi - \frac{1}{2}z\partial_z, \quad \eta_1 = \xi^2\partial_\xi + \xi z\partial_z, \quad (3.13)$$

with a barred sector given by $\xi \rightarrow \bar{\xi}$. These operators still satisfy the algebra eq. (3.7) under the Lie bracket. However, this algebra now admits a non-trivial extension

$$\eta_1 \rightarrow \xi^2\partial_\xi + \xi z\partial_z - z^2\partial_{\bar{\xi}}, \quad \bar{\eta}_1 \rightarrow \bar{\xi}^2\partial_{\bar{\xi}} + \bar{\xi} z\partial_z - z^2\partial_\xi, \quad (3.14)$$

which leaves the Lie brackets between all elements unchanged, and which vanishes in the boundary limit $z \rightarrow 0$. Using the extended algebra, and replacing \mathcal{O}_k by its dual field, the Casimir equation (3.10) becomes

$$(z\partial_z - z^2\partial_z^2 - 4z^2\partial_\xi\partial_{\bar{\xi}})\varphi = -\square_{\text{AdS}}\varphi = -m^2\varphi, \quad (3.15)$$

which is the Klein-Gordon equation for a massive scalar field in Poincaré AdS₃, with $m^2 = -\Delta_k(\Delta_k - 2)$ [33]. In the Δ_k scalar representation, the global conformal Casimir can be identified as the AdS₃ Laplacian, $\mathcal{C}_2 = -\square_{\text{AdS}}$.

In a similar manner, the Laplacian for the kinematic space of the CFT₂ vacuum state can be derived from the Casimir in an appropriate representation. The authors of [9] identified this representation from the transformation properties of OPE blocks, the natural candidates for fields on kinematic space. Under a conformal transformation, a spin-zero local operator with scaling dimension Δ_i transforms as

$$\mathcal{O}_i(x) \rightarrow \Omega(x')^{\Delta_i} \mathcal{O}_i(x'), \quad \Omega(x') = \det\left(\frac{\partial x'^\mu}{\partial x^\nu}\right), \quad (3.16)$$

while

$$|x_1 - x_2| \rightarrow (\Omega(x'_1)\Omega(x'_2))^{-1/2} |x'_1 - x'_2|. \quad (3.17)$$

From eq. (3.6), these transformation laws imply that OPE blocks obey

$$\mathcal{B}_k^{ij}(x_1, x_2) \rightarrow \left(\frac{\Omega(x'_1)}{\Omega(x'_2)}\right)^{(\Delta_i - \Delta_j)/2} \mathcal{B}_k^{ij}(x'_1, x'_2). \quad (3.18)$$

Restricting to the case of $\Delta_i = \Delta_j$ shows that the equal-weight OPE block transforms in a spinless, $\Delta = 0$ representation in each of its coordinates. This is the same transformation law as a pair of dimensionless scalar operators $\varphi_1(x_1)\varphi_2(x_2)$. The action of the conformal generators on this pair is, from eq. (3.8),

$$\begin{aligned} [L_n, \varphi_1(x_1)\varphi_2(x_2)] &= [L_n, \varphi_1(x_1)]\varphi_2(x_2) + \varphi_1(x_1)[L_n, \varphi_2(x_2)] \\ &= (\mathcal{L}_{n,1} + \mathcal{L}_{n,2})\varphi_1(x_1)\varphi_2(x_2), \end{aligned} \quad (3.19)$$

where $\mathcal{L}_{n,k}$ is the $\Delta = 0, l = 0$ differential representation of L_n acting only on the x_k coordinates. The OPE block is a linear combination of a single quasiprimary and its

descendants, so it satisfies a Casimir eigenvalue equation with the same eigenvalue (3.11) as the quasiprimary,

$$[\mathcal{C}_2, \mathcal{B}_k(x_1, x_2)] = -\frac{1}{2}(\mathcal{L}_1^{AB} + \mathcal{L}_2^{AB})(\mathcal{L}_{AB,1} + \mathcal{L}_{AB,2})\mathcal{B}_k(x_1, x_2) = C_k \mathcal{B}_k(x_1, x_2). \quad (3.20)$$

Employing an explicit representation for the conformal generators will produce a differential equation for the OPE blocks which can be interpreted as a Klein-Gordon equation on kinematic space.

From the global AdS₃ Killing vectors

$$\begin{aligned} \xi_{-1} &= \frac{1}{2}e^{-i(t+\phi)}(\tanh(\rho)\partial_t + i\partial_\rho + \coth(\rho)\partial_\phi), & \bar{\xi}_{-1} &= \frac{1}{2}e^{-i(t-\phi)}(\tanh(\rho)\partial_t + i\partial_\rho - \coth(\rho)\partial_\phi), \\ \xi_0 &= \frac{1}{2}(\partial_t + \partial_\phi), & \bar{\xi}_0 &= \frac{1}{2}(\partial_t - \partial_\phi), \\ \xi_1 &= \frac{1}{2}e^{i(t+\phi)}(\tanh(\rho)\partial_t - i\partial_\rho + \coth(\rho)\partial_\phi), & \bar{\xi}_1 &= \frac{1}{2}e^{i(t-\phi)}(\tanh(\rho)\partial_t - i\partial_\rho - \coth(\rho)\partial_\phi), \end{aligned} \quad (3.21)$$

we can obtain a differential representation of the conformal generators on the cylinder by taking the $\rho \rightarrow \infty$ boundary limit [31],

$$\begin{aligned} \mathcal{L}_{-1} &= \frac{1}{2}e^{-i(t+\phi)}(\partial_t + \partial_\phi), & \bar{\mathcal{L}}_{-1} &= \frac{1}{2}e^{-i(t-\phi)}(\partial_t - \partial_\phi), \\ \mathcal{L}_0 &= \frac{1}{2}(\partial_t + \partial_\phi), & \bar{\mathcal{L}}_0 &= \frac{1}{2}(\partial_t - \partial_\phi), \\ \mathcal{L}_1 &= \frac{1}{2}e^{i(t+\phi)}(\partial_t + \partial_\phi), & \bar{\mathcal{L}}_1 &= \frac{1}{2}e^{i(t-\phi)}(\partial_t - \partial_\phi). \end{aligned} \quad (3.22)$$

Using this representation to calculate the Casimir in its bilocal scalar representation (3.20) requires computing

$$-\frac{1}{2}\mathcal{L}_{AB,1}\mathcal{L}_1^{AB} - \frac{1}{2}\mathcal{L}_{AB,2}\mathcal{L}_2^{AB} + \mathcal{L}_{AB,1}\mathcal{L}_2^{AB}, \quad (3.23)$$

as in eq. (3.9). This task is simplified since the two terms which act on only a single coordinate do not contribute. This can be verified directly from the representation (3.22), or by noting that $L_{AB,i}L_i^{AB}$ acting on $\mathcal{B}_k(x_1, x_2)$ produces the eigenvalue (3.11), which vanishes for the $\Delta = 0$, $l = 0$ representation appropriate for the equal-weight OPE blocks in $d = 2$.

The term with mixed derivatives does not vanish. It is

$$\mathcal{L}_{AB,1}\mathcal{L}_2^{AB} = -4(\bar{\mathcal{L}}_{0,1}\bar{\mathcal{L}}_{0,2} + \mathcal{L}_{0,1}\mathcal{L}_{0,2}) + 2[\bar{\mathcal{L}}_{-1,1}\bar{\mathcal{L}}_{1,2} + \mathcal{L}_{1,1}\mathcal{L}_{-1,2} + \bar{\mathcal{L}}_{1,1}\bar{\mathcal{L}}_{-1,2} + \mathcal{L}_{-1,1}\mathcal{L}_{1,2}], \quad (3.24)$$

where the second index indicates which point in the pair (x_1, x_2) the operator acts on. Using eq. (3.22) leads to

$$\begin{aligned} \mathcal{L}_{AB,1}\mathcal{L}_2^{AB} &= -2(\partial_{t_1}\partial_{t_2} + \partial_{\phi_1}\partial_{\phi_2}) + \cos(t_1 - t_2 + \phi_1 - \phi_2)(\partial_{t_1} + \partial_{\phi_1})(\partial_{t_2} + \partial_{\phi_2}) \\ &\quad + \cos(t_1 - t_2 - (\phi_1 - \phi_2))(\partial_{t_1} - \partial_{\phi_1})(\partial_{t_2} - \partial_{\phi_2}). \end{aligned} \quad (3.25)$$

This operator simplifies greatly if we introduce coordinates analogous to the kinematic coordinates used in eq. (3.3),⁵

$$\begin{aligned}\alpha &= \frac{1}{2}(t_1 - t_2 + (\phi_1 - \phi_2)), & \theta &= \frac{1}{2}(t_1 + t_2 + \phi_1 + \phi_2), \\ \bar{\alpha} &= \frac{1}{2}(t_1 - t_2 - (\phi_1 - \phi_2)), & \bar{\theta} &= \frac{1}{2}(t_1 + t_2 - (\phi_1 + \phi_2)),\end{aligned}\tag{3.26}$$

which leads to

$$\mathcal{L}_{AB,1}\mathcal{L}_2^{AB} = -2\sin^2\alpha(-\partial_\alpha^2 + \partial_\theta^2) - 2\sin^2\bar{\alpha}(-\partial_{\bar{\alpha}}^2 + \partial_{\bar{\theta}}^2).\tag{3.27}$$

The Casimir equation for the OPE block is then

$$[\mathcal{C}_2, \mathcal{B}_k(x_1, x_2)] = [-2\sin^2\alpha(-\partial_\alpha^2 + \partial_\theta^2) - 2\sin^2\bar{\alpha}(-\partial_{\bar{\alpha}}^2 + \partial_{\bar{\theta}}^2)]\mathcal{B}_k(x_1, x_2) = \Delta_k(\Delta_k - 2)\mathcal{B}_k.\tag{3.28}$$

It is easy to check that this operator is the scalar Laplacian in the $dS_2 \times dS_2$ metric (3.4) found from conformal symmetry arguments. This motivates the interpretation of an OPE block as a negative mass scalar field propagating freely on kinematic space [9],

$$(\square_{dS} + \bar{\square}_{dS})\mathcal{B}_k(x_1, x_2) = m^2\mathcal{B}_k,\tag{3.29}$$

with the mass term $m^2 = -\Delta_k(\Delta_k - 2)$ given by the Casimir eigenvalue (3.11) for the quasiprimary of the block. Again, kinematic space is meant to be a useful auxiliary space, not a physical one, so the appearance of negative mass fields is not a concern.

In the following section the equal-time OPE will be considered for CFT's dual to conical defects. Setting $t_1 = t_2 = 0$ in eq. (3.26) and eliminating two redundant coordinates in eq. (3.28) leads to the Laplacian for a single dS_2 spacetime,

$$[\mathcal{C}_2, \mathcal{B}_k(t=0, \alpha, \theta)] = -4\sin^2\alpha\left(-\frac{\partial^2}{\partial\alpha^2} + \frac{\partial}{\partial\theta^2}\right)\mathcal{B}_k(t=0, \alpha, \theta).\tag{3.30}$$

3.3 CFT dual to conical defects

Conical defect spacetimes can be created by adding a particle to pure AdS and are dual to certain excited states of the boundary theory [25, 34]. The dual CFT is discretely gauged and lives on a cylinder with an angular identification inherited from the bulk. For the conical defects with integer N it is often useful to consider a covering CFT living on the boundary of pure AdS₃ that ungauges the discrete \mathbb{Z}_N symmetry [19].⁶ Physical, gauge invariant quantities in the base CFT can be computed from appropriately symmetrized quantities on the cover. This method of images on the cover is a common way to calculate correlation functions of operators in the base CFT [25, 36–39]. It is important to note that the covering CFT is not identical to the base CFT, as there are many non-symmetrized quantities on the cover that do not correspond to physical, gauge invariant quantities on the base. In addition, the two theories do not share the same central charge. In line

⁵There is no longer a tan because this transformation is between sets of coordinates on the cylinder.

⁶The covering CFT only inherits a Virasoro symmetry group when N is an integer [35].

with section 2, quantities on the base where $\tilde{\phi} \in [0, 2\pi/N]$ will be marked with a tilde to distinguish them from quantities on the cover where $\phi \in [0, 2\pi]$.

Restricting to integer N , a base operator $\tilde{\mathcal{O}}(t, \tilde{\phi})$ of dimension Δ can be represented on the cover by a symmetrized operator

$$\tilde{\mathcal{O}}(t, \tilde{\phi}) = \frac{1}{N} \sum_{m=0}^{N-1} \exp\left(i \frac{2\pi m}{N} \frac{\partial}{\partial \phi}\right) \mathcal{O}(t, \phi), \quad (3.31)$$

where $\mathcal{O}(t, \phi)$ is an operator on the cover of the same dimension Δ , with $\phi \in [0, 2\pi]$, and the first copy ($m = 0$) is inserted at $\phi = \tilde{\phi}$ by convention.⁷ This convention is somewhat arbitrary. It reflects the freedom to choose a fundamental domain on the kinematic space, as will become clear. The timelike coordinates of the two theories are simply identified, and we work on a fixed time slice in both cases. The generators of rotation

$$\exp\left(i \frac{2\pi m}{N} \frac{\partial}{\partial \phi}\right), \quad (3.32)$$

are conformal generators that have the effect of permuting through copies of $\mathcal{O}(t, \phi)$ equally spaced around the circle. An equivalent expression to eq. (3.31) is

$$\tilde{\mathcal{O}}(t, \tilde{\phi}) = \frac{1}{N} \sum_{m=0}^{N-1} \mathcal{O}\left(t, \phi + \frac{2\pi m}{N}\right). \quad (3.33)$$

3.3.1 Partial OPE block decomposition

The main goal of this section will be to obtain a symmetrized expression for the equal-time base OPE in terms of cover OPE blocks. That expression can then be used to determine the appropriate Casimir eigenvalue equation for the blocks, and in turn the kinematic space geometry can be inferred. The base OPE of equal-time operators inserted at locations $(t, \tilde{\phi}_1)$ and $(t, \tilde{\phi}_2)$ with $\tilde{\phi}_1 > \tilde{\phi}_2$ is of the form

$$\tilde{\mathcal{O}}_i(t, \tilde{\phi}_1) \tilde{\mathcal{O}}_j(t, \tilde{\phi}_2) = \left|2 - 2 \cos(\tilde{\phi}_1 - \tilde{\phi}_2)\right|^{-\Delta} \sum_k \tilde{C}_{ijk} \tilde{\mathcal{B}}_k(t, \tilde{\phi}_1, \tilde{\phi}_2), \quad (3.34)$$

where $\tilde{\mathcal{B}}_k(t, \tilde{\phi}_1, \tilde{\phi}_2)$ are the equal-time base OPE blocks.⁸ Again, $\Delta_i = \Delta_j = \Delta$ so the indices i, j on the OPE blocks are dropped for brevity. The base OPE can be rewritten using eq. (3.31), after which the OPE between cover operators can be broken into OPE

⁷The equality of scaling dimensions here is a consequence of unitarity in a 1+1d CFT and may not be guaranteed in higher dimensions.

⁸Here, operators on the cylinder have been rescaled relative to the planar operators used in section 3.2, see [40] for example. In the OPE limit $\tilde{\phi}_2 \rightarrow \tilde{\phi}_1$ where the curvature of the cylinder becomes unimportant, one recovers the form of eq. (3.6) for a planar CFT.

blocks to get

$$\begin{aligned}
\tilde{\mathcal{O}}_i(t, \tilde{\phi}_1) \tilde{\mathcal{O}}_j(t, \tilde{\phi}_2) &= \frac{1}{N^2} \sum_{a=0}^{N-1} \sum_{b=0}^{N-1} \exp\left(i \frac{2\pi a}{N} \frac{\partial}{\partial \phi_1}\right) \exp\left(i \frac{2\pi b}{N} \frac{\partial}{\partial \phi_2}\right) \mathcal{O}_i(t, \phi_1) \mathcal{O}_j(t, \phi_2) \\
&= \frac{1}{N^2} \sum_{a=0}^{N-1} \sum_{b=0}^{N-1} \exp\left(i \frac{2\pi a}{N} \frac{\partial}{\partial \phi_1}\right) \exp\left(i \frac{2\pi b}{N} \frac{\partial}{\partial \phi_2}\right) \\
&\quad \cdot \left[|2 - 2 \cos(\phi_1 - \phi_2)|^{-\Delta} \sum_k C_{ijk} \mathcal{B}_k(t, \phi_1, \phi_2) \right].
\end{aligned} \tag{3.35}$$

The structure constants and OPE blocks may be different on the cover compared to the base, and are differentiated by a tilde.

Now in the covering space we introduce kinematic coordinates of the form (cf. (3.26))

$$\alpha = \frac{1}{2}(\phi_1 - \phi_2), \quad \theta = \frac{1}{2}(\phi_1 + \phi_2). \tag{3.36}$$

The permutation generators can be rewritten

$$\exp\left(i \frac{2\pi a}{N} \frac{\partial}{\partial \phi_1}\right) \exp\left(i \frac{2\pi b}{N} \frac{\partial}{\partial \phi_2}\right) = \exp\left(i \frac{2\pi(a-b)}{N} \frac{\partial}{\partial \phi_1}\right) \exp\left(i \frac{2\pi b}{N} \frac{\partial}{\partial \theta}\right). \tag{3.37}$$

The N^2 terms in the double sum (3.35) can be reorganized into a more appealing form

$$\begin{aligned}
\tilde{\mathcal{O}}_i(t, \tilde{\phi}_1) \tilde{\mathcal{O}}_j(t, \tilde{\phi}_2) &= \\
&= \frac{1}{N^2} \sum_k C_{ijk} \sum_{m=0}^{N-1} \exp\left(i \frac{2\pi m}{N} \frac{\partial}{\partial \phi_1}\right) \left[|2 - 2 \cos(2\alpha)|^{-\Delta} \sum_{b=0}^{N-1} \exp\left(i \frac{2\pi b}{N} \frac{\partial}{\partial \theta}\right) \mathcal{B}_k(t, \alpha, \theta) \right].
\end{aligned} \tag{3.38}$$

The interior sum over b accounts for the N terms where both points ϕ_1 and ϕ_2 are shifted by the same amount, that is $a = b$. In this case α is fixed; the $\partial/\partial\theta$ generator permutes between images of the pair of operators on the cover. From the bulk viewpoint, $\partial/\partial\theta$ permutes through the N images of a geodesic that are identified under \mathbb{Z}_N . In the exterior sum, the $\partial/\partial\phi_1$ generators increase the angular distance between the insertion points. In bulk terms, $\partial/\partial\phi_1$ changes the winding number of geodesics connecting the boundary points.

It may seem more natural to use $\partial/\partial\alpha$ generators along with the $\partial/\partial\theta$ generators. However, when N is an even integer, acting with $\partial/\partial\alpha$ alone does not reach images on the cover of all separations α . In bulk terms, not all winding numbers for geodesics with a given orientation can be reached with $\partial/\partial\alpha$ generators alone. In order to reach all images for all integer N , a combination of $\partial/\partial\theta$ and one of $\partial/\partial\phi_1$ or $\partial/\partial\phi_2$ is needed, as illustrated in figure 4.

The form of eq. (3.38) suggests the definition of a more fine-grained OPE block which is symmetrized on the cover,

$$\mathcal{B}_{k,m}(t, \alpha, \theta) = \frac{1}{N} |2 - 2 \cos(2\alpha)|^{-\Delta} \sum_{b=0}^{N-1} \exp\left(i \frac{2\pi b}{N} \frac{\partial}{\partial \theta}\right) \mathcal{B}_k(t, \alpha, \theta), \tag{3.39}$$

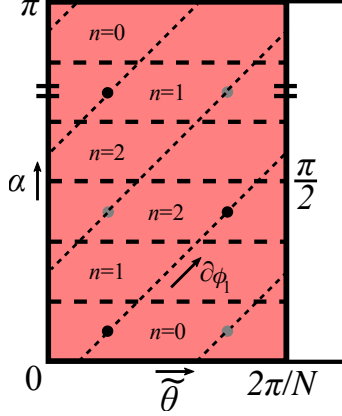


Figure 4: On kinematic space, ϕ_1 is a null coordinate. In terms of cover operators, acting with $\exp(i\frac{2\pi}{N}\frac{\partial}{\partial\phi_1})$ increases the angular separation α . In terms of conical defect geodesics, acting once with $\exp(i\frac{2\pi}{N}\frac{\partial}{\partial\phi_1})$ increases the winding number while leaving the endpoints fixed. All winding numbers are reached by acting with $\exp(i\frac{2\pi}{N}\frac{\partial}{\partial\phi_1})$ generators, in contrast to $\exp(i\frac{2\pi}{N}\frac{\partial}{\partial\alpha})$ generators.

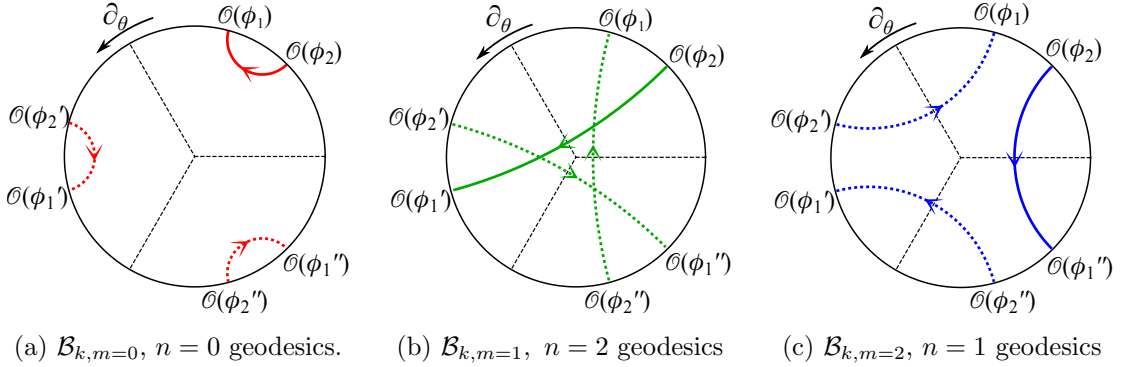


Figure 5: (a)-(c) The contributions to the base OPE from symmetrized pairs of operators at fixed angular separation in the covering CFT are encapsulated in the $\mathcal{B}_{k,m}$ blocks. The corresponding oriented bulk geodesics are displayed to show the pairings. Note that only two operators are inserted on the boundary at a time, but all image locations are displayed here for comparison.

where α takes on a fixed value α_m within each term of this block. We emphasize that since this “partial” OPE block is \mathbb{Z}_N symmetrized it is a valid observable on the base theory. The OPE of the base theory is then put in the suggestive form (cf. (3.31))

$$\tilde{\mathcal{O}}_i(t, \tilde{\phi}_1)\tilde{\mathcal{O}}_j(t, \tilde{\phi}_2) = \sum_k C_{ijk} \frac{1}{N} \sum_{m=0}^{N-1} \exp\left(i\frac{2\pi m}{N}\frac{\partial}{\partial\phi_1}\right) \mathcal{B}_{k,m}(t, \alpha_m, \theta). \quad (3.40)$$

The partial OPE blocks $\mathcal{B}_{k,m}(t, \alpha_m, \theta)$ encapsulate the contribution to the base OPE from ordered pairs of cover operators at a common distance $\alpha_m = \alpha + m\pi/N$, and $\phi_1 > \phi_2$ as in figure 5.

The base OPE blocks $\tilde{\mathcal{B}}_k$ in the decomposition (3.34) group the contributions to the OPE from the conformal family of the primary $\tilde{\mathcal{O}}_k$. In rearranging the sums to get (3.38) we lose this interpretation for the partial OPE blocks $\mathcal{B}_{k,m}(t, \alpha_m, \theta)$. It is not immediately

clear what CFT operator contributions these blocks group together. However, we will find that the partial OPE blocks have a clear interpretation in the bulk; they organize the contributions to the base OPE from bulk geodesics of fixed winding numbers.

For each block $\mathcal{B}_{k,m}(t, \alpha_m, \theta)$, the coordinate θ is in the domain $[0, 2\pi/N]$ since $\theta = \tilde{\theta}$ was set by convention. We can always choose θ in this fundamental domain, even though its full domain on the covering space is $[0, 2\pi]$, because the symmetry generators in eq. (3.39) permute through all the images of θ symmetrically. The choice of fundamental domain for this coordinate is the same as the choice for a fundamental domain of kinematic space made in eq. (2.17) and section 2.3.

Importantly, in a single $\mathcal{B}_{k,m}(t, \alpha_m, \theta)$ block the coordinate α_m is restricted to a domain of size $\pi/2N$. To see this, consider the $m = 0$ block where the image points have the smallest separation α and are connected by a geodesic of winding number $n = 0$ through the bulk. Fix ϕ_2 and allow ϕ_1 to take on different values. Keeping $n = 0$ and $\phi_1 > \phi_2$ requires ϕ_1 to stay in the domain $(\phi_2, \phi_2 + \pi/N)$. Over this domain $\alpha_{(m=0)} \in (0, \pi/2N)$ so the $\mathcal{B}_{k,0}$ block corresponds to α in this range. Increasing $m \rightarrow 1$ moves the ϕ_1 insertion to its next image at $\phi_1 + 2\pi/N$, so the $\mathcal{B}_{k,1}$ block has $\alpha_{(m=1)} \in (\pi/N, 3\pi/2N)$ and corresponds to geodesics of winding number $n = 2$. The relationship between m and n is piecewise linear, and differs for even or odd integer N . For odd N ,

$$N \text{ odd : } \begin{array}{|c|c|c|c|c|c|c|c|c|c|c|} \hline m & 0 & 1 & 2 & \dots & \lfloor N/2 \rfloor - 1 & \lfloor N/2 \rfloor & \lceil N/2 \rceil & \lceil N/2 \rceil + 1 & \dots & N-2 & N-1 \\ \hline n & 0 & 2 & 4 & \dots & N-3 & N-1 & N-2 & N-4 & \dots & 3 & 1 \\ \hline \end{array}, \quad (3.41)$$

while for even N ,

$$N \text{ even : } \begin{array}{|c|c|c|c|c|c|c|c|c|c|} \hline m & 0 & 1 & 2 & \dots & N/2 - 1 & N/2 & N/2 + 1 & \dots & N-2 & N-1 \\ \hline n & 0 & 2 & 4 & \dots & N-2 & N-1 & N-3 & \dots & 3 & 1 \\ \hline \end{array}. \quad (3.42)$$

All values of the winding number n are reached by the N applications of the $\partial/\partial\phi_1$ generator for both odd and even N . In summary, with our conventions each partial OPE block $\mathcal{B}_{k,m}(t, \alpha_m, \theta)$ lives in a restricted domain $\theta \in (0, 2\pi/N)$ and $\alpha_m \in (m\pi/N, m\pi/N + \pi/2N)$.

3.3.2 Partial OPE block Casimir equations

It was noted in eq. (3.20) that an OPE block satisfies a Casimir equation with the same eigenvalue as the quasiprimary \mathcal{O}_k it is built from. Since the Casimir operator commutes with all elements of the global conformal group, the $\mathcal{B}_{k,m}$ blocks satisfy the same Casimir equation as the \mathcal{B}_k blocks from which they are built (3.39), with the same eigenvalue,

$$\begin{aligned} [\mathcal{C}_2, \mathcal{B}_k(t, \alpha, \theta)] &= C_k \mathcal{B}_k, \\ \implies [\mathcal{C}_2, \mathcal{B}_{k,m}] &= \frac{1}{N} |2 - 2\cos(2\alpha)|^{-\Delta} \sum_{b=0}^{N-1} \exp\left(i \frac{2\pi b}{N} \frac{\partial}{\partial\theta}\right) [\mathcal{C}_2, \mathcal{B}_k] = C_k \mathcal{B}_{k,m}. \end{aligned} \quad (3.43)$$

The differential representation of \mathcal{C}_2 must be adapted for the $\mathcal{B}_{k,m}$ blocks compared to the $\tilde{\mathcal{B}}_k$ blocks because the conformal generators of the base and cover theory are not the same.

While the conical defect is dual to an excited state of the base CFT, the covering CFT is in its ground state [19]. For this reason, the differential form of the Casimir operator

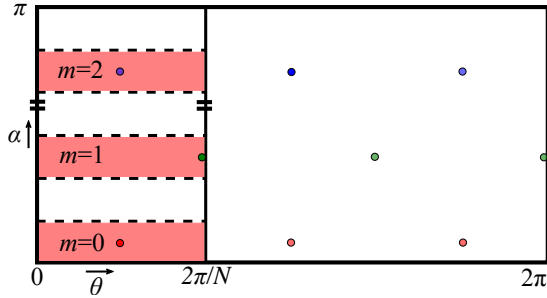


Figure 6: Individual $\mathcal{B}_{k,m}$ blocks give rise to one of the shaded regions of kinematic space. The corresponding geodesics from figure 5 are shown as points. The gaps are filled out by including contributions from the orientation reversed blocks with $\phi_1 < \phi_2$. These correspond to the orientation reversed versions of the geodesics in figure 5.

acting on the $\mathcal{B}_{k,m}$ blocks is given by eq. (3.23) using a representation such as in eq. (3.22). The only difference that appears in the calculation leading to the Laplacian on kinematic space, eq. (3.30), is the restricted coordinate domain of $\mathcal{B}_{k,m}(\alpha_m, \theta)$: $\theta \in (0, 2\pi/N)$ and $\alpha_m \in (m\pi/N, m\pi/N + \pi/2N)$. Thus the Casimir equation for the $\mathcal{B}_{k,m}$ blocks is

$$[\mathcal{C}_2, \mathcal{B}_{k,m}(t, \alpha_m, \theta)] = -4 \sin^2(\alpha_m) \left(-\frac{\partial^2}{\partial \alpha_m^2} + \frac{\partial^2}{\partial \theta^2} \right) \mathcal{B}_{k,m}(t, \alpha_m, \theta) = C_k \mathcal{B}_{k,m}(t, \alpha_m, \theta), \quad (3.44)$$

which suggests the metric for the kinematic space of the single $\mathcal{B}_{k,m}$ block is

$$ds_m^2 = \frac{1}{\sin^2 \alpha_m} (-d\alpha_m^2 + d\theta^2). \quad (3.45)$$

This is a subregion of dS_2 with the restricted coordinate range as indicated above. Each of the N $\mathcal{B}_{k,m}$ blocks gives rise to a region of kinematic space in the same vertical strip of width $\theta \in [0, 2\pi/N]$ but with differing ranges of α , as depicted in figure 6. The union of these N regions cover half of the vertical strip, but are not all connected because of how the winding number jumps as one insertion point is permuted through its images, recall tables (3.41) and (3.42). The indicated half of the vertical strip was obtained by taking $\phi_1 > \phi_2$ for the $m = 0$ block and acting with $\partial/\partial\phi_1$ generators. By starting with $\phi_1 < \phi_2$ for the $m = 0$ block and following the same construction with $\partial/\partial\phi_2$ in the place of $\partial/\partial\phi_1$, one fills out the remaining regions of kinematic space. This is made more clear with a view of the bulk picture in figure 5 where interchanging the roles of ϕ_1 and ϕ_2 reverses the orientation of the connecting geodesics.

The base OPE in eq. (3.40) receives contributions from each $\mathcal{B}_{k,m}$ with both $\phi_1 > \phi_2$ and $\phi_1 < \phi_2$. Taking the union of the regions identified from each $\mathcal{B}_{k,m}$ shows that the kinematic space for the excited states dual to a timeslice of $\text{AdS}_3/\mathbb{Z}_N$ can be identified as de Sitter with an identified angular coordinate $\theta = \theta + 2\pi/N$. In other words, the kinematic space of a static conical defect is a quotient of the kinematic space for pure AdS_3 , as anticipated in [8, 9, 28]. This is the same kinematic space geometry, up to the choice of fundamental region, that was determined from the differential entropy prescription of eq.

(2.17), and the analysis of boundary anchored geodesics under the \mathbb{Z}_N quotient in section 2.3.

Just as kinematic space from the bulk point of view can be divided into regions by the winding number of geodesics as in figure 2, from the CFT perspective kinematic space is built up from the contributions to the OPE by images of fixed separation α_m . This suggests that there should be a connection between the partial $\mathcal{B}_{k,m}$ OPE blocks and geodesics of a fixed winding number associated to m . This connection will be made explicit in the following section.

4 Discussion

In this paper we have shown that the kinematic space for a constant time slice of a static conical defect spacetime is a quotient of the kinematic space for time slices of pure AdS₃. This fact was anticipated in [9, 28, 41] since all locally AdS₃ spacetimes can be obtained as a quotient of AdS₃ itself, with geodesics of AdS₃ descending to geodesics of the quotient space. From the bulk our results were derived from the original differential entropy prescription, and by studying how the quotient acts on geodesics. The two approaches led to different subregions of the full dS₂ kinematic space for pure AdS₃, but it was argued that the subregions were equivalent fundamental domains under the identifications.

From the CFT point of view kinematic space had previously been defined as the space of ordered pairs of points. For a CFT dual to pure AdS₃ there is a one-to-one correspondence between ordered pairs of points and bulk geodesics, making it consistent with the bulk definition. Then, conformal symmetry can be used to derive a unique metric on the space of pairs of points, matching the bulk results. However, the one-to-one correspondence is not a typical feature of locally AdS₃ spacetimes. While the possibility of including non-minimal geodesics in the description of kinematic space has been considered previously from the bulk [22, 28, 41], there has been no clear generalization of the boundary point of view. In this paper we showed that the metric of the kinematic space for conical defects can be inferred from the Casimir equation of partial OPE blocks. Excited states in a discretely gauged CFT dual to conical defects can be related to the ground state of a covering CFT, and gauge invariant operators in base descend from symmetrized operators in the cover. This allows the base OPE blocks to be broken up into distinct contributions from pairs of image operators on the cover at each possible angular separation. These contributions are encapsulated in partial OPE blocks which were shown to satisfy a wave equation. The Laplacian appearing in the wave equation is that of a subregion of dS₂, which allows us to infer the metric of patches of kinematic space. The base OPE is a sum of partial OPE blocks, while the union of patches matches the kinematic space identified by bulk arguments.

The method of images provides the solution to the lack of a one-to-one correspondence between pairs of points and geodesics in this case. When both the bulk and boundary are lifted to their covering spaces, non-minimal geodesics become minimal geodesics connecting distinct image points. The fact that each partial OPE block corresponds to a specific range of α on the CFT covering space is very similar to how the α coordinate on kinematic space

arranges geodesics by their winding number. This suggests a holographic interpretation for the partial OPE blocks: the block $\mathcal{B}_{k,m}$ represents the contribution to the base OPE from a single class of bulk geodesics with fixed winding number n related to m by tables (3.41) or (3.42). Thus the partial OPE blocks allow for a more fine-grained understanding of the holographic contributions to the OPE. To confirm this suspicion we now consider the holographic dictionary entry relating OPE blocks and bulk fields integrated over geodesics that was established in [9], and find that partial OPE blocks are dual to bulk fields integrated over individual minimal or non-minimal geodesics.

4.1 Duality between OPE blocks and geodesic integrals of bulk fields

In [9] it was noted that a bulk scalar field integrated over a geodesic of AdS_3 satisfies the same differential equation on kinematic space as a scalar OPE block.⁹ By verifying that the two quantities also obeyed the same initial conditions a holographic dictionary entry was established for pure AdS_3 : *OPE blocks are dual to integrals of bulk local fields along geodesics.* The derivation of this dictionary entry relies heavily on the fact that both pure AdS_3 and its kinematic space $\text{dS}_2 \times \text{dS}_2$ are homogeneous spaces with the same isometry group. This allowed the authors to derive a kinematic space equation of motion for the integrated field by relating the action of the isometries on the field and on the geodesics. In contrast, the conical defect spacetimes are not homogeneous spaces. The defect traces out a worldline that is not invariant under boosts. Nevertheless, progress can be made on extending the dictionary entry to the conical defect case by working on the covering space. For continuity, we will review the essential points of the derivation of the dictionary entry in pure AdS_3 . Full details can be found in [9].

Consider a massive scalar field $\varphi_{\text{AdS}}(x)$ on AdS_3 integrated over a boundary anchored geodesic Γ in a constant time slice of the geometry,

$$R[\varphi_{\text{AdS}}](\Gamma) = \int_{\Gamma} ds \varphi_{\text{AdS}}(x). \quad (4.1)$$

This ‘‘X-ray’’ transform of $\varphi_{\text{AdS}}(x)$ is naturally viewed as a field on kinematic space because it is a function of geodesics, i.e. points in kinematic space.¹⁰

Let g be an isometry of AdS_3 . The scalar field is invariant under the isometry but its argument is shifted, $\varphi'_{\text{AdS}}(x) = \varphi_{\text{AdS}}(g^{-1} \cdot x)$. Integrating the shifted field over a geodesic Γ is equivalent to integrating the original field over a shifted geodesic $g \cdot \Gamma$, noting that all isometries of AdS_3 map geodesics into geodesics. In terms of the X-ray transform this is expressed as

$$R[\varphi'_{\text{AdS}}](\Gamma) = \int_{\Gamma} ds \varphi_{\text{AdS}}(g^{-1} \cdot x) = \int_{g \cdot \Gamma} ds \varphi_{\text{AdS}}(x) = R[\varphi_{\text{AdS}}](g \cdot \Gamma). \quad (4.2)$$

A shift in the argument of $\varphi_{\text{AdS}}(x)$ can be compensated by a shift in the argument of $R(\Gamma)$.

⁹See also [42, 43] for an independent development of the connection between geodesic operators and OPE blocks.

¹⁰When the integration is performed over an extremal surface in a higher dimensional theory this is known as a Radon transform, used first in a holographic context in [44].

When g is an element of the isometry group near the identity, the action of g on the field is described by the group generators

$$\varphi'_{AdS}(x) = (1 - \omega^{AB} L_{AB}^x) \varphi_{AdS}(x), \quad (4.3)$$

where L_{AB}^x is an isometry generator of AdS written with embedding space indices, and ω^{AB} is the antisymmetric matrix parameterizing the isometry. In a similar way, the action of g on the X-ray transform is

$$R[\varphi_{AdS}](g \cdot \Gamma) = (1 + \omega^{AB} L_{AB}^\Gamma) R[\varphi_{AdS}](\Gamma), \quad (4.4)$$

where L_{AB}^Γ is an isometry generator on the kinematic space of geodesics. Applying eqs. (4.3) and (4.4) to eq. (4.2) produces the remarkable intertwining relation of isometry generators

$$L_{AB}^\Gamma R[\varphi_{AdS}](\Gamma) = -R[L_{AB}^x \varphi_{AdS}](\Gamma). \quad (4.5)$$

Applying the same relation twice produces quadratic Casimirs (3.9), in their respective representations of the isometry group;

$$\mathcal{C}_2^\Gamma R[\varphi_{AdS}](\Gamma) = R[\mathcal{C}_2^x \varphi_{AdS}(x)](\Gamma). \quad (4.6)$$

The subsequent step of the derivation relies crucially on the properties of homogeneous spaces, as noted in [9]. For homogeneous spaces the Casimir operator of the isometry group is identified with the scalar Laplacian.¹¹ This was demonstrated for AdS₃ in eq. (3.15) and for dS₂ × dS₂ in eq. (3.28). On the right side of eq. (4.6) the Casimir acts on a scalar AdS field so the Casimir is in the bulk scalar representation $-\square_{AdS}$. On the left side the Casimir acts on a function of geodesics so it is in the kinematic space representation $-2(\square_{dS} + \bar{\square}_{dS})$. Using the equation of motion for the bulk field and the definition (4.1) leads to an equation of motion for the X-ray transform as a scalar field on kinematic space

$$2(\square_{dS} + \bar{\square}_{dS}) R[\varphi_{AdS}](\Gamma) = R[\square_{AdS} \varphi_{AdS}](\Gamma) = R[m^2 \varphi_{AdS}](\Gamma) = m^2 R[\varphi_{AdS}]. \quad (4.7)$$

This shows that free bulk scalars integrated over boundary anchored geodesics are free scalar fields propagating on kinematic space. This is the same equation satisfied by the OPE block (3.29) of a spin zero quasiprimary of dimension given by $-\Delta(\Delta - 2) = m^2$. The X-ray transform and OPE block also satisfy the same initial conditions on a Cauchy slice which establishes that they are dual quantities [9].

Conical defect case. Now let us analyze the conical defect case, again restricting to the quotients AdS₃/Z_N. The fact that conical defects are not homogeneous spaces precludes the possibility of running through the previous argument directly. However, it is possible

¹¹A homogeneous space can be written as the coset space of its isometry group quotiented by the stabilizer subgroup of a point. The Casimir of the isometry group is the scalar Laplacian for the group's Cartan-Killing metric. The same Laplacian is inherited by the coset space when the Casimir acts on functions that are constant on orbits of the stabilizer group. Note that a point in kinematic space is an AdS geodesic, so the stabiliser subgroup of a geodesic in AdS should be used in the quotient.

to use the intertwining relations obtained in the pure case and only then perform the \mathbb{Z}_N quotient with an appropriate prescription for the X-ray transform over conical defect fields.

Consider a massive bulk scalar field φ_{CD} on $\text{AdS}_3/\mathbb{Z}_N$, and similarly φ_{AdS} on pure AdS_3 , each described by the action

$$S = -\frac{1}{2} \int d^3x \sqrt{-g} ((\partial\varphi)^2 + m^2\varphi^2). \quad (4.8)$$

The Klein-Gordon equation in global coordinates, eq. (2.1) for pure AdS, and eq. (2.7) for the defect, is

$$\square\varphi = -\frac{1}{\cosh^2\rho} \partial_t^2\varphi + \frac{1}{\sinh^2\rho} \partial_\phi^2\varphi + \frac{1}{\cosh\rho\sinh\rho} \partial_\rho(\cosh\rho\sinh\rho\partial_\rho\varphi) = m^2\varphi. \quad (4.9)$$

For φ_{AdS} the angular coordinate is $\phi \in (0, 2\pi)$, while for φ_{CD} , ϕ should be replaced by $\tilde{\phi} \in (0, 2\pi/N)$.

In either case the solutions are obtained through separation of variables [37]. For example, in the AdS case solutions are $\varphi_{AdS}(t, \rho, \phi) = e^{i\omega t} Y_l(\phi) R(\rho)$, with the circular harmonics

$$Y_l(\phi) = e^{il\phi}, \quad Y_l(\phi + 2\pi n) = Y_l(\phi), \quad l, n \in \mathbb{Z}. \quad (4.10)$$

Similarly, $\varphi_{CD}(t, \rho, \tilde{\phi}) = e^{i\omega t} \tilde{Y}_m(\tilde{\phi}) R(\rho)$. The circular harmonic here is $2\pi/N$ periodic,

$$\tilde{Y}_m(\tilde{\phi}) = e^{iNm\tilde{\phi}}, \quad \tilde{Y}_m\left(\tilde{\phi} + \frac{2\pi n}{N}\right) = \tilde{Y}_m(\tilde{\phi}), \quad m, n \in \mathbb{Z}. \quad (4.11)$$

Therefore the φ_{CD} modes are a subset of the φ_{AdS} modes with $l = Nm$. They are \mathbb{Z}_N symmetric φ_{AdS} modes that are solutions of the conical defect Klein-Gordon equation in each \mathbb{Z}_N wedge of the covering space, reflecting the quotient structure of the defect. Appropriately symmetrized modes of AdS will be denoted $\varphi_{\mathbb{Z}}(\phi)$; any φ_{CD} can be obtained by restricting some $\varphi_{\mathbb{Z}}$ to a single \mathbb{Z}_N wedge.

The X-ray transform for the conical defect can then be defined as usual

$$R[\varphi_{CD}](\gamma) = \int_\gamma ds \varphi_{CD}(\tilde{x}). \quad (4.12)$$

However, this transform acts in a non-homogeneous space and may not share the same invertibility properties as its counterpart eq. (4.1). It is preferable to lift φ_{CD} and γ to the covering space where

$$R[\varphi_{CD}](\gamma) = \int_\gamma ds \varphi_{CD}(\tilde{x}) = \int_\Gamma ds \varphi_{\mathbb{Z}}(x) = R[\varphi_{\mathbb{Z}}](\Gamma). \quad (4.13)$$

Instead of integrating φ_{CD} over a geodesic γ in the conical defect spacetime, the corresponding symmetrized AdS field $\varphi_{\mathbb{Z}}$ can be integrated over one of the preimages Γ of γ under the \mathbb{Z}_N quotient, see figure 7. This prescription works for all boundary anchored γ , minimal or non-minimal, since all conical defect geodesics descend from geodesics Γ on AdS.

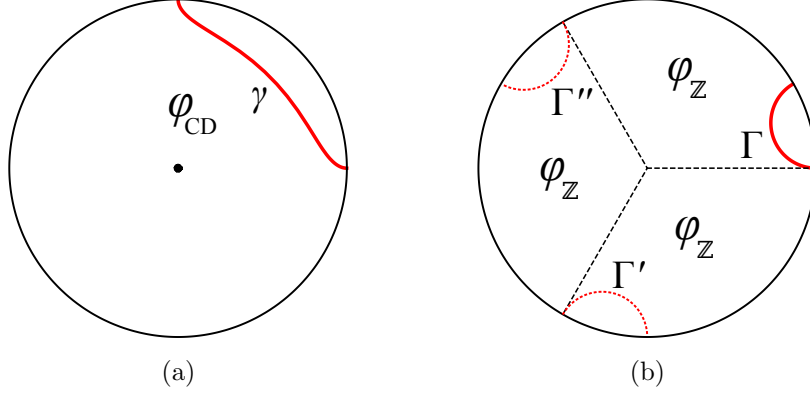


Figure 7: (a) A conical defect field integrated over a geodesic γ is the same as (b) a symmetrized AdS_3 field integrated over one of the preimages of γ under the \mathbb{Z}_N quotient. Identifying the edges of any wedge gives the conical defect of (a).

Note that in going from γ to Γ , and φ_{CD} to φ_Z in eq. (4.13) there is the freedom to choose one of several identical wedges. The choice of wedge will lead to different coordinate values for $\varphi_Z(\phi)$ and $\Gamma(\alpha, \theta)$. This is analogous to the ambiguities encountered throughout this paper in choosing a fundamental region. For consistency with the previous choice of a vertical strip of kinematic space, see figure 2, let Γ be the preimage of γ with the smallest centre angle which will always be in the range $\theta \in (0, 2\pi/N)$.

By working with the right side of eq. (4.13), the properties of homogeneous spaces can be used to find an intertwining relation for the equations of motion. Once again, let g be an infinitesimal isometry of AdS_3 . The intertwining relation eq. (4.5) for homogeneous spaces applies as before,

$$L_{AB}^\Gamma R[\varphi_Z](\Gamma) = -R[L_{AB}^x \varphi_Z](\Gamma), \quad (4.14)$$

and leads to the intertwined Casimirs

$$\mathcal{C}_2^\Gamma R[\varphi_Z](\Gamma) = R[\mathcal{C}_2^x \varphi_Z(x)](\Gamma). \quad (4.15)$$

On the right side the Casimir of AdS isometries becomes the AdS Laplacian which produces the mass eigenvalue. On the left side the Casimir is in the kinematic space representation $-2(\square_{dS} + \bar{\square}_{dS})$ so that

$$2(\square_{dS} + \bar{\square}_{dS})R[\varphi_Z](\Gamma) = m^2 R[\varphi_Z](\Gamma). \quad (4.16)$$

On both sides eq. (4.13) can be used to find the equation of motion for geodesic integrated fields on the conical defect

$$2(\square_{dS/\mathbb{Z}} + \bar{\square}_{dS/\mathbb{Z}})R[\varphi_{CD}](\gamma) = m^2 R[\varphi_{CD}](\gamma). \quad (4.17)$$

The notation $\square_{dS/\mathbb{Z}}$ is to remind that this operator now acts on the subspace of dS_2 obtained by restricting to $\theta \in (0, 2\pi/N)$ with periodic boundary conditions. This is the same behaviour that the symmetrized field exhibits under the quotient, namely $\square_{AdS} \varphi_{AdS}(x) = \square_{CD} \varphi_{CD}(\tilde{x})$ within any single wedge.

One might worry that the above argument leading to eq. (4.14) could break down when g is a boost isometry of AdS under which the conical defect is not invariant. Under the action of a boost, the field $\varphi_{\mathbb{Z}}(g^{-1} \cdot x)$ may no longer be symmetrized around the origin, but the conical defect no longer sits statically at the origin (see [38] for a relevant discussion). The moving defect is still locally AdS, and can be obtained directly from the covering AdS₃ spacetime through an identification along an AdS Killing vector. The identification is no longer a simple angular identification, but shifts time as well as angle. These identifications are given explicitly in [25, 45, 46] for example. The moving conical defect solutions can be viewed as global coordinate transformations of the static case, and do not exhibit any different physics compared to stationary ones. On an appropriately boosted timeslice through the moving conical defect spacetime, the transformed field $\varphi'_{CD}(\tilde{x})$ can be obtained from $\varphi'_{\mathbb{Z}}(x)$ using the identification that produces the spacetime itself.

The equation of motion for geodesic integrated fields on the conical defect, eq. (4.17), after taking the equal time limit is the same as the Casimir equation for the base OPE block $\tilde{\mathcal{B}}_k$. The OPE block $\tilde{\mathcal{B}}_k$ represents the contribution to the $\tilde{\mathcal{O}}_i \tilde{\mathcal{O}}_j$ OPE from the conformal family of the quasiprimary $\tilde{\mathcal{O}}_k$. From the bulk this contribution is obtained by integrating φ , the dual of $\tilde{\mathcal{O}}_k$, over *all* geodesics connecting the boundary insertion points of $\tilde{\mathcal{O}}_i$ and $\tilde{\mathcal{O}}_j$. This is the well known geodesic approximation which has been used to compute correlation functions [25, 38, 47], and geodesic Witten diagrams [7]. Non-minimal geodesics provide a finite number of sub-leading corrections to the minimal geodesic contribution, but can become significant in some regimes.

The connection between bulk and boundary can be made more detailed through the use of kinematic space. Consider the case where γ is a minimal geodesic. The X-ray transform $R[\varphi_{CD}](\gamma_{\min})$ over a minimal $\gamma(\tilde{\alpha}, \tilde{\theta})$, is restricted to $\tilde{\alpha} \in (0, \pi/2N)$, $\tilde{\theta} \in (0, 2\pi/N)$ with periodicity in the $\tilde{\theta}$ coordinate. The appropriate wave equation (4.17) on the $t = 0$ timeslice is

$$4 \sin^2 \tilde{\alpha} \left(-\frac{\partial^2}{\partial \tilde{\alpha}^2} + \frac{\partial^2}{\partial \tilde{\theta}^2} \right) R[\varphi_{CD}](\gamma) = m^2 R[\varphi_{CD}](\gamma). \quad (4.18)$$

Comparing with eq. (3.44) suggests that the $\mathcal{B}_{k,m}$ block with $m = 0$ is dual to $R[\varphi_{CD}](\gamma_{\min})$ and represents the contribution to the base OPE from a single class of geodesics, the minimal ones. The duality between $\mathcal{B}_{k,0}$ and $R[\varphi_{CD}](\gamma_{\min})$ is established by showing that these quantities satisfy the same initial conditions. The $\tilde{\alpha} = 0$ Cauchy slice of kinematic space is obtained by taking the coincidence limit of the OPE block, and in the bulk by integrating over a small geodesic that stays near the boundary. These limits are unchanged from the pure AdS case and have been discussed previously [7, 9, 29]. In the coincidence limit only the quasiprimary \mathcal{O}_k on the cover, and not its descendants, contributes to the partial OPE block

$$\lim_{\alpha \rightarrow 0} \mathcal{B}_{k,0}(\alpha, \theta) = \lim_{\alpha \rightarrow 0} |2\alpha|^{\Delta_k} \mathcal{O}_k(\theta), \quad (4.19)$$

while in the conical defect spacetime the behaviour of the dual scalar field near the AdS boundary is given by the extrapolate dictionary

$$\lim_{\rho \rightarrow \infty} \varphi_{CD}(t = 0, \rho, \tilde{\phi}) = \rho^{-\Delta_k} \mathcal{O}_k(\tilde{\phi}), \quad (4.20)$$

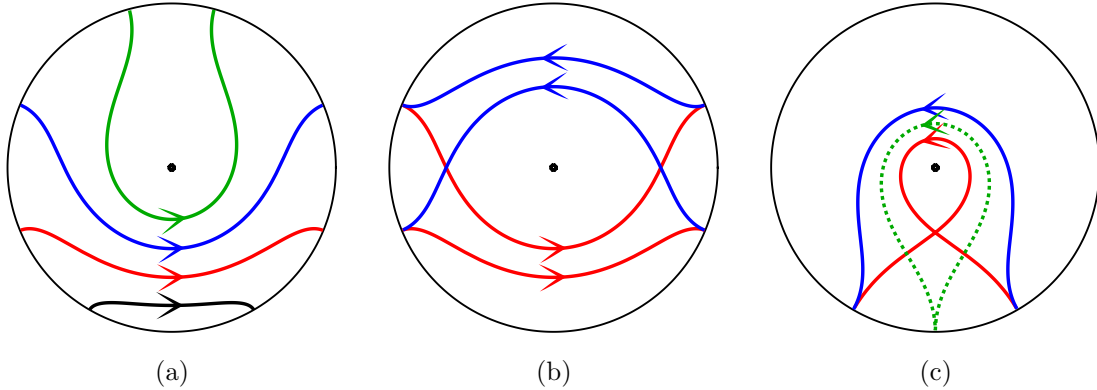


Figure 8: (a) Oriented geodesics away from the defect are continuous in length and shape as their opening angle is increased. (b) Geodesics with the same endpoints but different orientation cannot be smoothly transformed into one another across the defect. (c) As the opening angle of the blue geodesic increases it reaches the dashed geodesic. The red geodesic also reaches the dashed geodesic as its opening angle decreases, showing continuous behaviour even as the winding number jumps.

so that integrating over a small geodesic localized at $\tilde{\phi} = \tilde{\theta}$ gives

$$\lim_{\tilde{\alpha} \rightarrow 0} R[\varphi_{CD}](\gamma_{\min}(\tilde{\alpha}, \tilde{\theta})) = \lim_{\tilde{\alpha} \rightarrow 0} \frac{\Gamma(\Delta_k/2)^2}{2\Gamma(\Delta_k)} |2\tilde{\alpha}|^{\Delta_k} \mathcal{O}_k(\tilde{\theta}). \quad (4.21)$$

Hence, the initial conditions on kinematic space provide the relative normalization between the dual quantities,

$$R[\varphi_{CD}](\gamma_{\min}(\tilde{\alpha}, \tilde{\theta})) = \frac{\Gamma(\Delta_k/2)^2}{2\Gamma(\Delta_k)} \mathcal{B}_{k,0}(\alpha, \theta). \quad (4.22)$$

In general, the $\mathcal{B}_{k,m}$ block represents the contribution to the base OPE from the dual field φ_{CD} integrated over geodesics with winding number n , where m and n are related by table (3.41) or (3.42). For the non-minimal cases with $n \geq 1$, the geodesics do not stay near the boundary, preventing the use of eq. (4.20). However, the transition between winding numbers is smooth. Away from the defect it is clear that there is no discontinuity in the length or shape of *oriented* geodesics as $\tilde{\alpha}$ is increased, even as the winding number jumps, see figure 8. This means the X-ray transform $R[\varphi_{CD}](\gamma)$ is a continuous and smooth function of the bulk geodesics on the $\tilde{\alpha} < \pi/2$ region of kinematic space. Similarly, the partial OPE blocks $\mathcal{B}_{k,m}$ blocks defined in eq. (3.39) are continuous in $\tilde{\alpha}$ across transitions in the winding number. This is simply because the OPE behaves smoothly as the operator insertions are moved, and it remains convergent for all separations [40].

There is a potential obstacle to the continuity of $R[\varphi_{CD}](\gamma)$ at $\tilde{\alpha} = \pi/2$ where geodesics touch the defect. Geodesics in AdS_3 with $\tilde{\alpha} = \pi/2$ pass through the origin and behave smoothly as $\tilde{\alpha}$ is varied, but the corresponding geodesics on the defect spacetime must jump as they pinch in on the defect. As depicted in figure 9, geodesics with constant center angle $\tilde{\theta}$ jump as $\tilde{\alpha}$ is increased past $\pi/2$ and are not homologous across the jump. Despite this, the length and shape of such geodesics varies smoothly which suggests the X-ray transform of φ_{CD} will be smooth as well. That this must be the case is easiest to

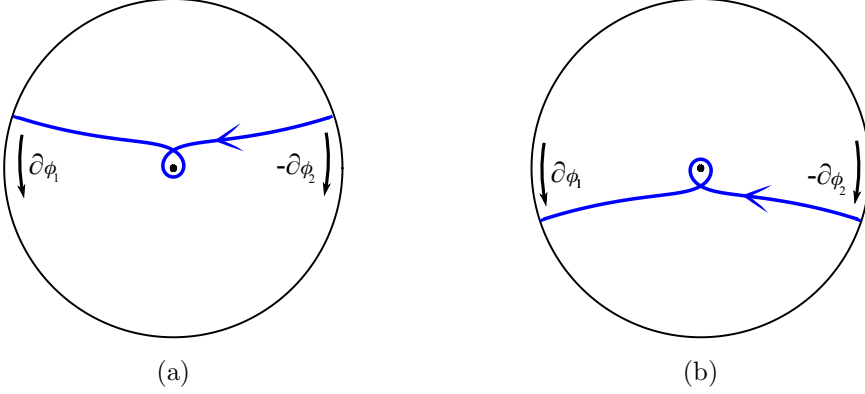


Figure 9: Geodesics in AdS_3 with $\alpha = \pi/2$ pass through the origin, and descend to geodesics which touch the conical defect. On AdS_3 , the behaviour of such geodesics is completely smooth as α is varied, but on the defect spacetime the endpoints may jump as (a) $\alpha = \pi/2 - \epsilon$ increases to (b) $\alpha = \pi/2 + \epsilon$ with $\tilde{\theta}$ held constant. This will be the case when N is not an odd integer. Despite this, the length and shape of such geodesics varies smoothly.

see by using the lifted X-ray transform (4.13). There is no discontinuity whatsoever in the transform of lifted geodesics as α is increased past $\pi/2$.

One can avoid this obstacle entirely by considering an alternative Cauchy slice on the upper half of kinematic space, namely $\tilde{\alpha} = \pi$, which also corresponds to near-boundary geodesics and the coincidence limit for the OPE. By the same argument made for $\tilde{\alpha} = 0$, the X-ray transform $R[\varphi_{CD}](\gamma)$ over a minimal geodesic with $\tilde{\alpha} \in ((1 - 1/2N)\pi, \pi)$ obeys the same initial conditions as the corresponding partial OPE block, and both are continuous functions on the $\tilde{\alpha} > \pi/2$ half of kinematic space.

Since the initial conditions in the $\tilde{\alpha} \rightarrow 0, \pi$ limits match between $\mathcal{B}_{k,m}$ and $R[\varphi_{CD}](\gamma)$, the equations of motion (3.44) and (4.17) along with continuity in $\tilde{\alpha}$ establish the duality between OPE blocks and geodesic operators for static conical defects. The base OPE receives contributions from each bulk geodesic, minimal and non-minimal, connecting the boundary insertion points. Each partial OPE block encapsulates the contribution to the base OPE from the dual bulk field integrated over a single geodesic of fixed winding number.

4.2 Future directions

The various approaches to kinematic space used in this paper were adapted to constant time slices of the bulk geometry, equivalently the equal-time limit of the OPE. In each case it was seen that the conical defect kinematic space was a quotient of the pure AdS_3 kinematic space using the same quotient that produces the conical defect from AdS_3 . The full four dimensional geometry of kinematic space describing the time dependent bulk [9] should also be obtainable using this quotient. There will be a new ambiguity, in addition to the choice of fundamental regions discussed in this paper, from the possibility of rotating in time the faces of AdS_3 which are identified, see for example figure 1 from [46]. On neighbouring constant time slices of the AdS_3 geometry the wedge representing the conical defect spacetime can have a relative shift in its angular coordinate. The kinematic spaces for

subsequent time slices would be vertical strips of dS_2 with different ranges of centre angle θ . Since the twisted and untwisted identifications of AdS_3 produce physically identical conical defect spacetimes, this extra ambiguity can be resolved by making a canonical prescription for an appropriate fundamental region of kinematic space. A complete description of this ambiguity is left for future work.

The CFT results in this paper were derived in the special case dual to AdS_3/\mathbb{Z}_N , since there is a particularly simple description of this system in terms of a covering CFT in its vacuum state. It is not surprising that the CFT descriptions of the integer and non-integer cases are significantly different when the holographic consequences are kept in mind. The integer defect spacetimes in the bulk have a mild orbifold singularity that does not obstruct the construction of a consistent string theory on this background [36, 48, 49].¹²

Furthermore, this paper was only concerned with static conical defects. These are part of a more general class of moving defects which are produced either by boosting the static solution, or by taking a quotient of AdS_3 along a Killing vector with a timelike component [25, 38, 45, 46]. It would be interesting to perform this quotient on the AdS_3 kinematic space to obtain the kinematic space of a moving defect. Then, using the relation between OPE blocks and geodesic bulk fields it may be possible to use the method of images to relate back to results on the geodesic approximation for correlation function in those spacetimes.

The partial OPE blocks discussed in this paper reorganize the operator contributions to the base OPE as compared to the traditional OPE blocks. While a clean CFT interpretation of the operator grouping in terms of conformal families is lost, we gain a bulk interpretation in terms of the contributions of geodesics with different winding numbers. It would be enlightening to understand better the CFT operator contributions that are represented by partial OPE blocks. One potential avenue to explore is the superficially similar construction used in [50]. Our partial OPE blocks were constructed by first un-gauging a discrete symmetry in going to the covering space description. Gauge invariance is restored by considering symmetrized sums of cover operators under the action of the \mathbb{Z}_N symmetry. The authors of [50] studied conformal blocks which give the contribution of a conformal family to a four-point function. The blocks were approximated by considering only the contribution from light descendants at the cost of modular invariance for the four-point function. Modular invariance was restored by summing over images of the approximate block under the action of modular generators. It may be that these two constructions are related on a deeper level.¹³

The sum over descendants composing an OPE block evinces that they are non-local operators in the CFT. As such, OPE blocks $\mathcal{B}_k(x_1, x_2)$ have a smeared representation where the quasi-primary \mathcal{O}_k they are built from is integrated over a causal diamond defined by the insertion points x_1, x_2 [9, 29]. It was suggested in [9] that for conical defects the OPE blocks corresponding to winding geodesics should have a smeared representation over diamonds which wrap all the way around the CFT cylinder (See figure 20 of [9]). Indeed, our cover OPE blocks have a smeared representation over causal diamonds on the covering

¹²We thank Oleg Lunin for comments on this point.

¹³We thank the referee for commenting on this similarity.

CFT cylinder, and so partial OPE blocks can be viewed as symmetrized sums over smeared operators on the cover (3.39). For the block $\mathcal{B}_{k,0}$ representing minimal geodesics, the causal diamonds on the cover are each contained within one \mathbb{Z}_N portion of the cylinder and do not overlap. For blocks representing winding geodesics, the causal diamonds extend over multiple \mathbb{Z}_N portions and can overlap with each other (cf. figure 5b). Imposing the \mathbb{Z}_N angular identification on any one of these large causal diamonds produces a diamond which wraps around the cylinder of the base CFT and can overlap on itself. It would be interesting to know if the CFT avatar of entwinement [19, 21] can be cast in terms of partial OPE blocks and wrapping diamonds, and how the bulk can be probed in a more fine-grained fashion using these objects.

Other locally AdS₃ geometries and their kinematic spaces have been studied from the bulk and using the differential entropy definition [22, 28, 41, 51], but differences in definitions for kinematic space have led to inconsistent results. For instance, the geometries for the kinematic space of the BTZ black holes described in [22] include geodesics of both orientations, while [28] and [51] do not. Furthermore, the authors of [28] chose to include only minimal geodesics in their definition of kinematic space, in contrast to the choice we have made here. In this paper we have advocated for defining kinematic space from the CFT in terms of OPE blocks and have isolated the important contributions of non-minimal geodesics. Valuable lessons about the equivalence and applicability of the various kinematic space definitions could be learned by applying this approach to the BTZ case and understanding the kinematic space independently from an OPE block perspective. Work along these directions is in progress.

To date, kinematic space has mainly been used to examine general features of AdS/CFT that can be constrained by conformal symmetry alone. It would be interesting to apply the kinematic space proposal to a particular realization of AdS/CFT. For instance, one could study a chiral primary state in the D1-D5 CFT in the limit where it is dual to a conical defect in the bulk [34].

Acknowledgments

The authors wish to thank James Sully for a fruitful seminar visit, Ian T. Jardine for collaboration in the initial stages of the project, as well as Zaq Carson and Oleg Lunin for useful discussions. The work of JCC and AWP is supported by a Discovery Grant from the Natural Sciences and Engineering Research Council of Canada. JCC is also supported by an Ontario Graduate Scholarship and a Vanier Canada Graduate Scholarship.

References

- [1] J. Maldacena, *The large- N limit of superconformal field theories and supergravity*, *International Journal of Theoretical Physics* **38** (1999) 1113–1133, [[hep-th/9711200](#)].
- [2] E. Witten, *Anti de Sitter space and holography*, *Adv.Theor.Math.Phys.* **2**: (1998) 253–291, [[hep-th/9802150](#)].
- [3] S. Gubser, I. Klebanov and A. Polyakov, *Gauge theory correlators from non-critical string theory*, *Physics Letters B* **428** (May, 1998) 105–114, [[hep-th/9802109](#)].

- [4] S. Ferrara, A. F. Grillo and R. Gatto, *Manifestly conformal covariant operator-product expansion*, *Lettere al Nuovo Cimento (1971-1985)* **2** (1971) 1363–1369.
- [5] S. Ferrara, A. Grillo, G. Parisi and R. Gatto, *Covariant expansion of the conformal four-point function*, *Nuclear Physics B* **49** (1972) 77 – 98.
- [6] E. Hijano, P. Kraus and R. Snively, *Worldline approach to semi-classical conformal blocks*, *JHEP* **2015** (2015) 131, [[1501.02260](#)].
- [7] E. Hijano, P. Kraus, E. Perlmutter and R. Snively, *Witten diagrams revisited: the AdS geometry of conformal blocks*, *JHEP* **2016** (2016) 146, [[1508.00501v2](#)].
- [8] B. Czech, L. Lamprou, S. McCandlish and J. Sully, *Integral geometry and holography*, *JHEP* **2015** (2015) 175, [[1505.05515v1](#)].
- [9] B. Czech, L. Lamprou, S. McCandlish, B. Mosk and J. Sully, *A stereoscopic look into the bulk*, *JHEP* **2016** (2016) 129, [[1604.03110v2](#)].
- [10] J. de Boer, M. P. Heller, R. C. Myers and Y. Neiman, *Holographic de sitter geometry from entanglement in conformal field theory*, *Phys. Rev. Lett.* **116** (Feb, 2016) 061602, [[1509.00113](#)].
- [11] W. Donnelly and S. B. Giddings, *Diffeomorphism-invariant observables and their nonlocal algebra*, *Phys. Rev. D* **93** (Jan, 2016) 024030, [[1507.07921](#)].
- [12] W. Donnelly and S. B. Giddings, *Observables, gravitational dressing, and obstructions to locality and subsystems*, *Phys. Rev. D* **94** (Nov, 2016) 104038, [[1607.01025](#)].
- [13] S. Ryu and T. Takayanagi, *Holographic derivation of entanglement entropy from the anti-de Sitter space/conformal field theory correspondence*, *Phys. Rev. Lett.* **96** (May, 2006) 181602, [[hep-th/0603001](#)].
- [14] V. Balasubramanian, B. D. Chowdhury, B. Czech, J. de Boer and M. P. Heller, *Bulk curves from boundary data in holography*, *Phys. Rev. D* **89** (Apr, 2014) 086004, [[1310.4204](#)].
- [15] S. Bhowmick, S. Das and B. Ezhuthachan, *Entanglement entropy and kinematic space in BCFT*, [[1703.01759v2](#)].
- [16] M. Bañados, C. Teitelboim and J. Zanelli, *Black hole in three-dimensional spacetime*, *Phys. Rev. Lett.* **69** (Sep, 1992) 1849–1851, [[hep-th/9204099](#)].
- [17] M. Bañados, M. Henneaux, C. Teitelboim and J. Zanelli, *Geometry of the 2+1 black hole*, *Phys. Rev. D* **48** (Aug, 1993) 1506–1525, [[gr-qc/9302012](#)].
- [18] S. Deser, R. Jackiw and G. 't Hooft, *Three-dimensional Einstein gravity: Dynamics of flat space*, *Annals of Physics* **152** (1984) 220 – 235.
- [19] V. Balasubramanian, B. D. Chowdhury, B. Czech and J. de Boer, *Entwinement and the emergence of spacetime*, *JHEP* **2015** (2015) 48, [[1406.5859v2](#)].
- [20] B. Freivogel, R. A. Jefferson, L. Kabir, B. Mosk and I.-S. Yang, *Casting shadows on holographic reconstruction*, *Phys. Rev. D* **91** (Apr, 2015) 086013, [[1412.5175](#)].
- [21] V. Balasubramanian, A. Bernamonti, B. Craps, T. De Jonckheere and F. Galli, *Entwinement in discretely gauged theories*, *JHEP* **2016** (Dec, 2016) 94, [[1609.03991](#)].
- [22] J.-d. Zhang and B. Chen, *Kinematic space and wormholes*, *JHEP* **2017** (2017) 92, [[1610.07134v2](#)].

- [23] R. C. Myers, J. Rao and S. Sugishita, *Holographic holes in higher dimensions*, *JHEP* **2014** (Jun, 2014) 44, [[1403.3416v2](#)].
- [24] R. Espíndola, A. Guijosa, A. Landetta and J. F. Pedraza, *What's the point? hole-ography in Poincaré AdS*, [1708.02958v1](#).
- [25] V. Balasubramanian and S. F. Ross, *Holographic particle detection*, *Phys. Rev. D* **61** (Jan, 2000) 044007, [[hep-th/9906226v1](#)].
- [26] C. T. Asplund, A. Bernamonti, F. Galli and T. Hartman, *Holographic entanglement entropy from 2d CFT: heavy states and local quenches*, *JHEP* **2015** (2015) 171, [[1410.1392](#)].
- [27] B. Czech and L. Lamprou, *Holographic definition of points and distances*, *Phys. Rev. D* **90** (Nov, 2014) 106005, [[1409.4473v1](#)].
- [28] C. T. Asplund, N. Callebaut and C. Zukowski, *Equivalence of emergent de Sitter spaces from conformal field theory*, *JHEP* **2016** (2016) 154, [[1604.02687](#)].
- [29] J. de Boer, F. M. Haehl, M. P. Heller and R. C. Myers, *Entanglement, holography and causal diamonds*, *JHEP* **2016** (2016) 1–83, [[1606.03307](#)].
- [30] A. Karch, J. Sully, C. F. Uhlemann and D. G. E. Walker, *Boundary kinematic space*, *JHEP* **2017** (Aug, 2017) 39, [[1703.02990v1](#)].
- [31] J. D. Brown and M. Henneaux, *Central charges in the canonical realization of asymptotic symmetries: An example from three dimensional gravity*, *Communications in Mathematical Physics* **104** (Jun, 1986) 207–226.
- [32] F. Dolan and H. Osborn, *Conformal partial waves and the operator product expansion*, *Nuclear Physics B* **678** (2004) 491 – 507, [[hep-th/0309180](#)].
- [33] J. Maldacena and A. Strominger, *Ads 3 black holes and a stringy exclusion principle*, *JHEP* **1998** (1998) 005, [[hep-th/9804085](#)].
- [34] O. Lunin, S. D. Mathur and A. Saxena, *What is the gravity dual of a chiral primary?*, *Nuclear Physics B* **655** (2003) 185 – 217, [[hep-th/0211292](#)].
- [35] J. de Boer, M. M. Sheikh-Jabbari and J. Simón, *Near-horizon limits of massless BTZ and their CFT duals*, *Classical and Quantum Gravity* **28** (2011) 175012, [[1011.1897v2](#)].
- [36] V. Balasubramanian, A. Naqvi and J. Simón, *A multi-boundary AdS orbifold and DLCQ holography: a universal holographic description of extremal black hole horizons*, *JHEP* **2004** (2004) 023, [[hep-th/0311237](#)].
- [37] I. Y. Aref'eva and M. A. Khramtsov, *AdS/CFT prescription for angle-deficit space and winding geodesics*, *JHEP* **2016** (2016) 121, [[1601.02008v2](#)].
- [38] I. Y. Aref'eva, M. A. Khramtsov and M. D. Tikhonovskaya, *Improved image method for a holographic description of conical defects*, *Theoretical and Mathematical Physics* **189** (2016) 1660–1672, [[1604.08905](#)].
- [39] I. Y. Aref'eva, M. A. Khramtsov and M. D. Tikhonovskaya, *Thermalization after holographic bilocal quench*, *JHEP* **2017** (Sep, 2017) 115, [[1706.07390](#)].
- [40] D. Pappadopulo, S. Rychkov, J. Espin and R. Rattazzi, *Operator product expansion convergence in conformal field theory*, *Phys. Rev. D* **86** (Nov, 2012) 105043, [[1208.6449](#)].
- [41] B. Czech, L. Lamprou, S. McCandlish and J. Sully, *Tensor networks from kinematic space*, *JHEP* **2016** (2016) 100, [[1512.01548](#)].

- [42] B. C. da Cunha and M. Guica, *Exploring the BTZ bulk with boundary conformal blocks*, [1604.07383v1](#).
- [43] M. Guica, *Bulk fields from the boundary OPE*, *Nordita-2016-144* (2016) , [[1610.08952v2](#)].
- [44] J. Lin, M. Marcolli, H. Ooguri and B. Stoica, *Locality of gravitational systems from entanglement of conformal field theories*, *Phys. Rev. Lett.* **114** (Jun, 2015) 221601, [[1412.1879](#)].
- [45] H.-J. Matschull, *Black hole creation in 2 + 1 dimensions*, *Classical and Quantum Gravity* **16** (1999) 1069, [[gr-qc/9809087](#)].
- [46] I. Areféva, A. Bagrov, P. Säterskog and K. Schalm, *Holographic dual of a time machine*, *Phys. Rev. D* **94** (Aug, 2016) 044059, [[1508.04440](#)].
- [47] K. Goto and T. Takayanagi, *CFT descriptions of bulk local states in the AdS black holes*, *JHEP* **2017** (Oct, 2017) 153, [[1704.00053v1](#)].
- [48] S. Giusto, O. Lunin, S. D. Mathur and D. Turton, *D1-D5-P microstates at the cap*, *JHEP* **2013** (Feb, 2013) 50, [[1211.0306](#)].
- [49] J. Son, *String theory on AdS₃/Z_n*, *HUTP-01/A034* (2001) , [[hep-th/0107131v1](#)].
- [50] A. Maloney, H. Maxfield and G. S. Ng, *A conformal block farey tail*, *JHEP* **2017** (Jun, 2017) 117, [[1609.02165](#)].
- [51] B. Czech, G. Evenbly, L. Lamprou, S. McCandlish, X.-l. Qi, J. Sully et al., *Tensor network quotient takes the vacuum to the thermal state*, *Phys. Rev. B* **94** (Aug, 2016) 085101, [[1510.07637](#)].